



## OPEN ACCESS

## EDITED BY

Ciria Hernandez,  
University of Michigan, United States

## REVIEWED BY

Daohua Jiang,  
Institute of Physics (CAS), China  
Samuel Goodchild,  
Xenon Pharmaceuticals Inc., Canada

## \*CORRESPONDENCE

Markus Rapedius  
markus.rapedius@nanion.de

†These authors have contributed  
equally to this work

## SPECIALTY SECTION

This article was submitted to  
Molecular Signalling and Pathways,  
a section of the journal  
Frontiers in Molecular Neuroscience

RECEIVED 30 June 2022

ACCEPTED 26 July 2022

PUBLISHED 22 August 2022

## CITATION

Rapedius M, Obergrussberger A,  
Humphries ESA, Scholz S,  
Rinke-Weiss I, Goetze TA, Brinkwirth N,  
Rotordam MG, Strassmaier T,  
Randolph A, Friis S, Liutkute A,  
Seibertz F, Voigt N and Fertig N (2022)  
There is no F in APC: Using  
physiological fluoride-free solutions  
for high throughput automated patch  
clamp experiments.  
*Front. Mol. Neurosci.* 15:982316.  
doi: 10.3389/fnmol.2022.982316

## COPYRIGHT

© 2022 Rapedius, Obergrussberger,  
Humphries, Scholz, Rinke-Weiss,  
Goetze, Brinkwirth, Rotordam,  
Strassmaier, Randolph, Friis, Liutkute,  
Seibertz, Voigt and Fertig. This is an  
open-access article distributed under  
the terms of the [Creative Commons  
Attribution License \(CC BY\)](https://creativecommons.org/licenses/by/4.0/). The use,  
distribution or reproduction in other  
forums is permitted, provided the  
original author(s) and the copyright  
owner(s) are credited and that the  
original publication in this journal is  
cited, in accordance with accepted  
academic practice. No use, distribution  
or reproduction is permitted which  
does not comply with these terms.

# There is no F in APC: Using physiological fluoride-free solutions for high throughput automated patch clamp experiments

Markus Rapedius<sup>1\*†</sup>, Alison Obergrussberger<sup>1†</sup>,  
Edward S. A. Humphries<sup>2</sup>, Stephanie Scholz<sup>1</sup>,  
Ilka Rinke-Weiss<sup>1</sup>, Tom A. Goetze<sup>1</sup>, Nina Brinkwirth<sup>1</sup>,  
Maria Giustina Rotordam<sup>1</sup>, Tim Strassmaier<sup>3</sup>,  
Aaron Randolph<sup>3</sup>, Søren Friis<sup>1</sup>, Aiste Liutkute<sup>4,5,6</sup>,  
Fitzwilliam Seibertz<sup>4,5,6</sup>, Niels Voigt<sup>4,5,6</sup> and Niels Fertig<sup>1</sup>

<sup>1</sup>Nanion Technologies GmbH, Munich, Germany, <sup>2</sup>Discovery Sciences, BioPharmaceuticals R&D, AstraZeneca, Cambridge, United Kingdom, <sup>3</sup>Nanion Technologies Inc., Livingston, NJ, United States, <sup>4</sup>Institute of Pharmacology and Toxicology, University Medical Center Göttingen, Georg-August University, Göttingen, Germany, <sup>5</sup>German Center for Cardiovascular Research, Partner Site Göttingen, Göttingen, Germany, <sup>6</sup>Cluster of Excellence "Multiscale Bioimaging: From Molecular Machines to Networks of Excitable Cells", University of Göttingen, Göttingen, Germany

Fluoride has been used in the internal recording solution for manual and automated patch clamp experiments for decades because it helps to improve the seal resistance and promotes longer lasting recordings. In manual patch clamp, fluoride has been used to record voltage-gated Na (Na<sub>v</sub>) channels where seal resistance and access resistance are critical for good voltage control. In automated patch clamp, suction is applied from underneath the patch clamp chip to attract a cell to the hole and obtain a good seal. Since the patch clamp aperture cannot be moved to improve the seal like the patch clamp pipette in manual patch clamp, automated patch clamp manufacturers use internal fluoride to improve the success rate for obtaining GΩ seals. However, internal fluoride can affect voltage-dependence of activation and inactivation, as well as affecting internal second messenger systems and therefore, it is desirable to have the option to perform experiments using physiological, fluoride-free internal solution. We have developed an approach for high throughput fluoride-free recordings on a 384-well based automated patch clamp system with success rates >40% for GΩ seals. We demonstrate this method using hERG expressed in HEK cells, as well as Na<sub>v</sub>1.5, Na<sub>v</sub>1.7, and

K<sub>Ca</sub>3.1 expressed in CHO cells. We describe the advantages and disadvantages of using fluoride and provide examples of where fluoride can be used, where caution should be exerted and where fluoride-free solutions provide an advantage over fluoride-containing solutions.

#### KEYWORDS

automated patch clamp, ion channels, hERG, Na<sub>v</sub>1.5, physiological solutions, K<sub>Ca</sub>3.1, Na<sub>v</sub>1.7, fluoride

## Introduction

Automated patch clamp (APC) instruments are used for a wide variety of applications ranging from basic research into channelopathies and biophysical characteristics of ion channels, through to routine cardiac safety testing (Obergrussberger et al., 2021, 2022). Their use in cardiac safety screening has increased over the years and APC is now an established and accepted technique in most, if not all, safety testing laboratories. It is well-known that fluoride is often used in the internal solution in APC experiments to improve the seal resistance (Zeng et al., 2008) when external calcium (or other divalent cation) are present (Milligan et al., 2009; Obergrussberger et al., 2014, 2018). The mechanism is thought to involve the formation of CaF<sub>2</sub> crystals at the interface between the pipette or micro-pore and the cell as described in a recent patent application (Lojkner et al., 2019). Even in manual patch clamp experiments, fluoride has been used to record Na<sub>v</sub> channels for over 20 years (Cummins et al., 1999; Renganathan et al., 2000; Rugiero et al., 2003), despite known shifts in activation and steady-state inactivation curves of Na<sub>v</sub>1.9 (Rugiero et al., 2003; Coste et al., 2004), effects on the voltage dependence of conductance and steady-state inactivation of Na<sub>v</sub>1.7 (Jarecki et al., 2008), shifts in activation and inactivation of Na<sub>v</sub>1.3 (Meadows et al., 2002), and effects on persistent current of Na<sub>v</sub>1.3 (Chen et al., 2000). These effects on biophysical properties are not limited to Na<sub>v</sub> channels, high concentrations of fluoride have been shown to increase mean open duration, and thereby open probability of L-type calcium channels (Ono and Arita, 1999), and influences current amplitude and inactivation of K<sub>v</sub>1.3 and K<sub>2P</sub> channels (Herrmann et al., 2020). In addition to effects on biophysical properties of ion channels, fluoride binds to calcium making its use in experiments involving activation of ion channels by internal free calcium somewhat limited, and itself activates certain ion channels such as CFTR (Berger et al., 1998). It is also well-known that fluoride activates G-proteins when complexed with Al<sup>3+</sup> present in trace amounts (Li, 2003) and inhibits protein phosphatase (Khatra and Soderling, 1978). Fluoride is used because it improves the seal and allows stable measurements to be performed over long periods of time (Zeng et al., 2008; Föhr et al., 2021). Alternative internal solutions

which do not contain fluoride for recording CFTR (Billet et al., 2017; Froux et al., 2020; Becq et al., 2021) or TMEM16A (Obergrussberger et al., 2018) have been used successfully on automated patch clamp devices, but the solutions were not always physiological.

In most experiments run on automated patch clamp instruments, the use of fluoride in the internal solution is no problem, particularly when like is compared with like, i.e., activation and inactivation plots of Na<sub>v</sub> channels are always run using internal fluoride. However, there may be some cases where fluoride-free, physiological solutions are required, for example, when comparing data with historical data which was recorded in fluoride-free solutions. Alternatively, it may be the case that fluoride cannot be used because of activation of ion channels, inhibition of phosphatase or binding of calcium ions. For these reasons, we have developed a method for high throughput APC experiments using the SyncroPatch 384 which allow fluoride-free, physiological solutions to be used with good success rates for GΩ and sub-GΩ seals. We demonstrate this using the ion channels Na<sub>v</sub>1.5 and Na<sub>v</sub>1.7 expressed in CHO (Charles River), hERG expressed in HEK293 (SB Drug Discovery), and K<sub>Ca</sub>3.1 (SK4) also expressed in CHO cells (Charles River). Additionally, preliminary experiments using human induced pluripotent stem cell-derived cardiomyocytes (hiPSC-CMs) were also performed.

## Materials and methods

### Cell culture and harvesting

The cell lines used here (hERG stably expressed in HEK 293 cells from SB Drug Discovery, Glasgow, United Kingdom, hNa<sub>v</sub>1.5; hNa<sub>v</sub>1.7, and K<sub>Ca</sub>3.1 stably expressed in CHO cells all from Charles River, United States) were cultured as previously described (Brueggemann et al., 2004; Brüggemann et al., 2008; Becker et al., 2013; Obergrussberger et al., 2014). In brief, these cells were cultured in T175 culture flasks in the media recommended by the supplier and passaged every 2–3 days when they were 50–80% confluent. The cells were passaged regularly to ensure that the cells were single when passaged and harvested. The cells were prohibited from reaching 100%

confluency so that they remained healthy, single, and expressed the ion channel of interest when they were harvested into a cell suspension for recordings. hiPSC-derived cardiomyocytes were generated and cultured as previously described (Seibert et al., 2022). Briefly, hiPSC cell line UMGi014-C.14 was derived from dermal fibroblasts of healthy male donor and the reprogramming to iPSCs was achieved using integration-free CytoTune iPS 2.0 Sendai Reprogramming Kit (Thermo Fisher Scientific) with the reprogramming factors OCT4, KLF4, SOX2, c-MYC. Directed differentiation into ventricular iPSC-CMs was performed *via* WNT signaling modulation and subsequent metabolic selection, as previously described (Kleinsorge and Cyganek, 2020). hiPSC-CMs were cultured at 37°C in 5% CO<sub>2</sub> in a RPMI Medium 1640 (1X) + GlutaMax™ -I [+]  
25 mM HEPES (Thermo Fisher Scientific) supplemented with B-27 (Thermo Fisher Scientific). Experiments were performed on hiPSC-CMs at day 41 post differentiation. All protocols were approved by the Ethics Committee of the University Medical Center Göttingen (No. 10/9/15 and 15/2/20). For experiments on the SyncroPatch 384, cells were harvested into suspension and suction was used to attract a cell to the patch clamp aperture of each well. Since it was a blind method for capture, cells had to be single with few clusters and the cell suspension was free from cell debris, as the presence of cell clusters and debris can decrease the success rate. Cell harvesting was performed as described previously (Brueggemann et al., 2004; Brüggemann et al., 2008; Becker et al., 2013; Obergrussberger et al., 2014) using TrypLE, other suitable enzymes, or even enzyme-free detachment protocols. Cells were then resuspended in extracellular recording solution at a density of ~500,000 cells/ml.

## Automated patch clamp electrophysiology

All cells were recorded in the whole cell mode of the patch clamp technique using the SyncroPatch 384 (Nanion Technologies, Munich, Germany). Electrophysiological protocols were constructed, and data digitized using PatchControl 384 (Nanion Technologies, Munich, Germany). Cells were recorded on both single-hole NPC-384 or NPC-384FF chips with medium or high resistance (4–5.5 or 5–7 MΩ, respectively). In a subset of experiments involving K<sub>Ca</sub>3.1 multi-hole chips with 4 holes (NPC-384/NPC-384FF) 4X high resistance (2.2–3.2 MΩ) per well were used. Cells were harvested into suspension and added to the CellHotel of the SyncroPatch 384 where they were kept at 10°C, shaking at 200 rpm, until used for the experiment. The NPC-384 or NPC-384FF chips were filled with internal solution as indicated in Table 1 and ChipFill external solution. After cells were captured (indicated by an increase in R<sub>Seal</sub> > 10 MΩ), a brief, transient addition of external solution containing 6 mM Ca<sup>2+</sup> was made when standard internal solution and NPC-384 chips were used

which was then exchanged to external recording solution before commencement of recordings. When fluoride-free internal solution and NPC-384FF chips were used, the ChipFill external solution was replaced by external recording solution (Table 1) after cells were captured.

hERG currents were recorded using a double step voltage protocol from a holding potential of -80 mV to +60 mV for 500 ms followed by a step to -40 mV for 500 ms repeated every 15 s. Peak amplitude was measured at the start of the second voltage step (I<sub>Tail</sub>). Current-voltage relationships were recorded using the same voltage-step to +60 mV, but then followed by voltage steps from -120 to 60 mV with 10 mV increments.

Na<sub>V</sub>1.5 currents were measured using a 3-step protocol, the first step from -120 to 0 mV, the second step from -100 to 0 mV and the 3rd step from -80 to 0 mV, repeated every 10 s. Current-voltage (IV) relationships were recorded using the voltage-step protocol: For the activation IV, a step pulse of 30 ms was applied, starting from -70 mV and increasing in 10 mV increments up to 40 mV with every sweep, at a sweep interval of 2 s. For analysis, the current response to each step was normalized to the cell's peak current before averaging across all cells. Holding potential was -120 mV.

The inactivation IV pulse protocol consisted of a 500 ms pre-pulse, starting from -100 mV and increasing in 5 mV increments with every sweep up to 20 mV, followed by a 50 ms depolarizing step to 0 mV, at a sweep interval of 5 s. For analysis, each of the current responses to the 50 ms step to 0 mV was normalized to the current response to the 0 mV step following the 500 ms pre-pulse at -120 mV before averaging across all cells. Holding potential was -120 mV.

K<sub>Ca</sub>3.1 was recorded using a voltage ramp protocol from -120 to +60 mV over 198 ms, intersweep holding potential was -80 mV and sweep interval was 5 s. K<sub>Ca</sub>3.1 was activated by internal perfusion of free calcium at 0.3, 1, or 3 μM calculated using Cabuf (freeware from KU Leuven, Belgium).

Ca<sub>V</sub> currents from hiPSC-CMs were recorded using a voltage ramp-step protocol, with a ramp from -80 to -40 mV over 300 ms followed by a step from -40 to 0 mV for 100 ms, holding potential was -80 mV. The ramp section of the protocol was used to inactivate Na<sub>V</sub> currents. Only the current response to the step to 0 mV is shown in the figure for hiPSC-CMs.

Each well of the SyncroPatch 384 has an individual headstage of the amplifier and, therefore, each well is denoted as *n* = 1. For success rate and IC<sub>50</sub> values across plates, *n* represents results from 1 NPC-384 chip. With PatchControl 384, parameters such as seal resistance, capacitance and series resistance were determined from each well after application of a test pulse. All parameters are monitored over time and can be recorded for individual experiments.

## Method of using fluoride-free physiological solutions on the SyncroPatch 384

To allow for fluoride-free recordings, a combinatory approach is adopted on the SyncroPatch 384 consisting

**TABLE 1** Composition of recording solutions for fluoride-containing (referred to as standard internal) and fluoride-free (referred to as FF internal) experiments.

Constituent	Internal recording solution			External recording solution	ChipFill external solution (divalent-free)
	Standard	Standard-K <sub>Ca</sub> 3.1*	FF	Standard (incl. K <sub>Ca</sub> 3.1)/FF	Standard (incl. K <sub>Ca</sub> 3.1)/FF
K-gluconate		30	120		
K-Fluoride	120	80			
NaCl	10	10	10	80	140
NMDG-Cl				60	
KCl	10	10	10	4	4
CaCl <sub>2</sub>				2	
MgCl <sub>2</sub>				1	
EGTA	5	10	5		
Glucose				5	5
HEPES	10	10	10	10	10
pH	7.2	7.2	7.2	7.4	7.4
Osmolarity (mOsm)	~285	~285	~285	~289	~289

Concentrations are given in mM. Note that for experiments involving K<sub>Ca</sub>3.1, CaCl<sub>2</sub> was added to the internal solution as described in Section “Automated patch clamp electrophysiology.”  
\*In recordings with free [Ca<sup>2+</sup> > 1 μM] 10 mM HEDTA was used instead of EGTA.

of the usage of a specialized, fluoride-free consumable called NPC-384FF in combination with a proprietary, fully automated method for preparing the NPC-384FF prior to execution of the fluoride-free recording. The automated method of NPC-384FF preparation is available on all SyncroPatch 384 devices.

### Quality control parameters

Cells had to pass quality control (QC) parameters to be included in the analysis. For some experiments  $R_{Seal} > 1 \text{ G}\Omega$  whereas for other experiments  $R_{Seal} > 0.25 \text{ G}\Omega$  was used for single- or equivalent in multi-hole chips. In addition to this,  $I_{Peak} > 150 \text{ pA}$  for hERG;  $I_{Peak} < -100 \text{ pA}$  for Nav1.5 or Nav1.7 and  $I_{Peak} > 350 \text{ pA}$  for single-hole chips and  $I_{Peak} > 1000 \text{ pA}$  for multi-hole chips (4X) for K<sub>Ca</sub>3.1 was also used. In order to guarantee appropriate voltage clamp in our comparisons, the analysis of IV-relationships for Nav1.5 and Nav1.7 recordings included additional quality control parameters on capacitance  $> 2 \text{ pF}$ , current size as well as  $R_{Series}$  that was constrained to  $-3.0 \text{ nA}$  and  $20 \text{ M}\Omega$ , respectively.

### Automated patch clamp solutions

See [Table 1](#).

### Data analysis

The SyncroPatch 384 platforms have a software package consisting of PatchControl 384 (for data acquisition) and DataControl 384 (for data analysis; both Nanion Technologies, Munich, Germany). Current-voltage plots were calculated using DataControl 384 and fit with Boltzmann

equations:  $I(V) = I_{min} + \frac{I_{max}-I_{min}}{1 + e^{-\frac{V-V_{half}}{Slope}}}$  for a sigmoidal fit for hERG IV and inactivation Nav1.5 and Nav1.7 IVs. In addition, an extended Boltzmann equation was used:  $G(V) = \frac{I(V)}{V-E_{rev}} = \left( G_{min} + \frac{G_{max}-G_{min}}{1 + e^{-\frac{V-V_{half}}{Slope}}} \right)$  to obtain  $V_{half}$  values for activation protocols for Nav1.5 and Nav1.7 where  $I(V)$  is the amplitude of the current and  $G(V)$  the conductance at voltage  $V$ ,  $E_{rev}$  is the reversal potential.  $V_{half}$  is the membrane potential at half-maximal activation or inactivation and  $Slope$  is the slope factor.

Concentration response curves were calculated using either cumulative additions or a single point addition approach. When cumulative additions were done, all concentrations of compound were added to each well, in increasing concentrations, and concentration response curves were calculated individually for each well. When single point additions were done, a single concentration of compound was added to each well and the IC<sub>50</sub> was calculated across multiple wells. IC<sub>50</sub> analysis was done with DataControl 384, concentration response curves were fit with a Hill equation:

$$Response = Min + \frac{Max-Min}{1 + \left(\frac{EC_{50}}{Conc.}\right)^{Hill}}$$

### Statistics

Data are presented as means  $\pm$  S.D or means  $\pm$  S.E.M. Differences between groups were tested using the Student's

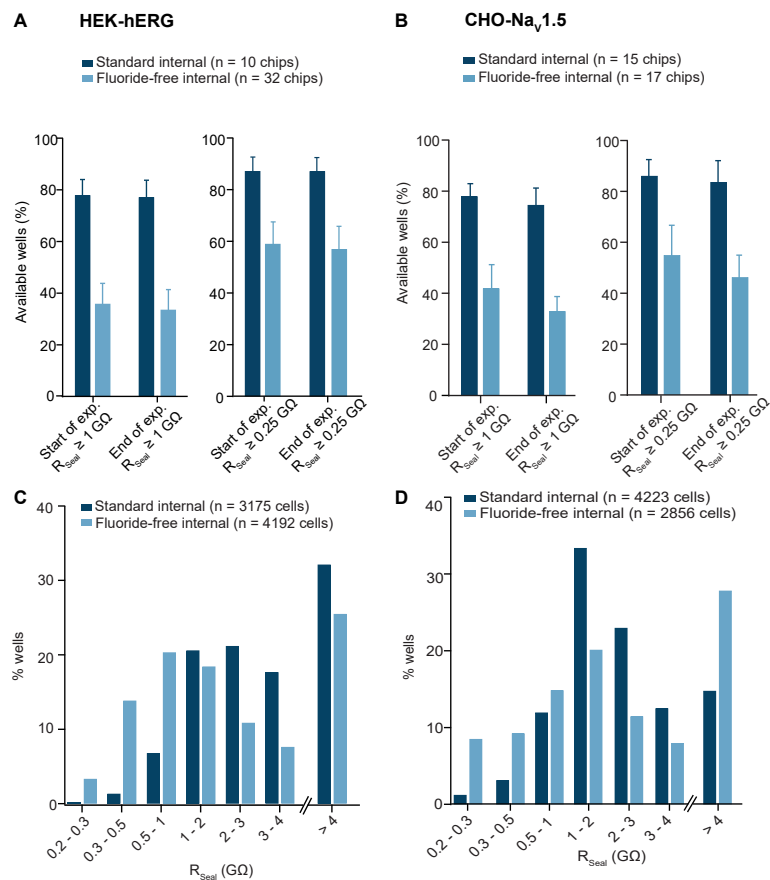


FIGURE 1

HEK and CHO cells recorded in standard and fluoride-free internal solution. **(A)** HEK cells expressing hERG were captured with almost 80% success rate for  $R_{Seal} \geq 1 \text{ G}\Omega + I_{Tail} > 150 \text{ pA}$  and almost 40% success rate for  $R_{Seal} \geq 1 \text{ G}\Omega$  in fluoride-free internal solution (left). If a QC cutoff of  $R_{Seal} \geq 0.25 \text{ G}\Omega + I_{Tail} > 150 \text{ pA}$  was used, the success rate was increased in both conditions (right). **(B)** CHO cells expressing  $Na_v1.5$  were captured with almost 80% success rate for  $R_{Seal} \geq 1 \text{ G}\Omega + I_{Peak} < -100 \text{ pA}$  and over 40% success rate for  $R_{Seal} \geq 1 \text{ G}\Omega$  in fluoride-free internal solution (left). If a QC cutoff of  $R_{Seal} \geq 0.25 \text{ G}\Omega + I_{Peak} < -100 \text{ pA}$  was used, the success rate was increased in both conditions (right). **(C)** Histogram plot of the  $R_{Seal}$  values for HEK-hERG cells in standard and fluoride-free internal solution. For  $R_{Seal} > 4 \text{ G}\Omega$ , although they are high giga-seals, the seal resistance is not accurately calculated and is therefore shown as an extra bar and these  $R_{Seal}$  values were not included in the calculation for  $R_{Seal}$  (Table 2). **(D)** Histogram plot of the  $R_{Seal}$  values for CHO- $Na_v1.5$  cells in standard and fluoride-free internal. For  $R_{Seal} > 4 \text{ G}\Omega$ , although they are high giga-seals, the seal resistance is not accurately calculated and is therefore shown as an extra bar and these  $R_{Seal}$  values were not included in the calculation for  $R_{Seal}$  (Table 3).

TABLE 2 Parameters for  $R_{Seal}$ ,  $I_{Tail}$ , cell capacitance,  $R_{Series}$ , Rundown,  $V_{half}$ , and  $IC_{50}$  values for HEK cells expressing hERG for standard internal and fluoride-free internal solution.

Parameter	Standard internal	Fluoride-free internal
$R_{Seal}$ (GΩ)	2.23 ± 0.02 (2155)	1.36 ± 0.02 (3123)*
$I_{Tail}$ (nA)	0.70 ± 0.01 (3175)	0.99 ± 0.01 (4192)***
Capacitance (pF)	16.2 ± 0.3 (387)	15.9 ± 0.4 (313)
$R_{Series}$ (MΩ)	8.6 ± 0.2 (379)	10.2 ± 0.2 (317)***
Rundown over 18 min (%/min)	0.10 ± 0.05 (58)	0.07 ± 0.07 (42)
$V_{half}$ (mV)	-93.0 ± 0.5 (190)	-92.1 ± 2.3 (261)
$IC_{50}$ Terfenadine (nM)	237 ± 26 (52)	337 ± 53 (17)
$IC_{50}$ Verapamil (nM)	394 ± 17 (54)	457 ± 37 (29)

$R_{Seal}$  values > 4 GΩ could not be accurately calculated, therefore only  $R_{Seal} \leq 4 \text{ G}\Omega$  were used for the calculation of the mean. Shown are mean ± S.E.M, number of cells shown in parentheses.

\* $P < 0.05$ , \*\*\* $P < 0.001$ , unpaired Student's *t*-test.

**TABLE 3** Parameters for  $R_{\text{Seal}}$ ,  $I_{\text{Peak}}$ , rundown,  $V_{\text{half}}$  Activation,  $V_{\text{half}}$  Inactivation, and tetracaine  $IC_{50}$  for CHO cells expressing Nav1.5 for standard internal and fluoride-free internal solution.

Parameter	Standard internal	Fluoride-free internal
$R_{\text{Seal}}$ (G $\Omega$ )	1.89 $\pm$ 0.02 (3598)	1.39 $\pm$ 0.02 (2061)***
$I_{\text{Peak}}$ (nA)	-1.56 $\pm$ 0.01 (4537)	-1.53 $\pm$ 0.01 (3336)
Capacitance (pF)	13.9 $\pm$ 0.2 (1043)	13.8 $\pm$ 0.4 (491)
$R_{\text{Series}}$ (M $\Omega$ )	7.6 $\pm$ 0.1 (1043)	9.8 $\pm$ 0.1 (491)***
Rundown over 12 min (%/min; $V_{\text{hold}}$ -120 mV)	0.5 $\pm$ 0.1 (133)	0.4 $\pm$ 0.1 (52)
$V_{\text{half}}$ Activation (mV)	-37.5 $\pm$ 0.4 (484)	-25.2 $\pm$ 0.5 (241)***
$V_{\text{half}}$ Inactivation (mV)	-68.4 $\pm$ 0.4 (728)	-53.6 $\pm$ 0.6 (165)***
$IC_{50}$ Tetracaine ( $\mu$ M, $V_{\text{hold}}$ -120 mV)	35.6 $\pm$ 9.4 (4 chips)	41.8 $\pm$ 9.3 (3 chips)

$R_{\text{Seal}}$  values > 4 G $\Omega$  could not be accurately calculated, therefore only  $R_{\text{Seal}} \leq 4$  G $\Omega$  were used for the calculation. Shown are mean  $\pm$  S.E.M, number of cells shown in parentheses. For tetracaine concentration response curves, single point additions were made and the concentration response curve calculated across the whole chip. Shown are mean  $\pm$  S.E.M for the number of chips given in parentheses.

\*\*\* $P < 0.001$ , unpaired Student's  $t$ -test.

$t$ -test for normally distributed data.  $P$ -values are reported in the figures.  $N$  represents the number of wells examined or the number of chips as indicated in the figures and/or figure legends.

## Results

### High throughput automated patch clamp to assess effects of internal fluoride on success rate and seal resistance

In APC experiments, high success rates have been reported using internal solutions without fluoride for several targets, such as CFTR, with success rates for completed experiments > 80% (Billet et al., 2017; Brüggemann et al., 2017; Froux et al., 2020; Becq et al., 2021). However, when switching to more physiological solutions, such as K-chloride or K-gluconate-based internal solutions, success rates very rarely reach acceptable ranges for high throughput APC. In fact, under these conditions we observed  $9.3 \pm 6.1\%$  ( $R_{\text{Seal}} > 1$  G $\Omega$  +  $I_{\text{Tail}} > 150$  pA) and  $18.6 \pm 6.3\%$  ( $R_{\text{Seal}} > 0.25$  G $\Omega$  +  $I_{\text{Tail}} > 150$  pA) using hERG expressed in HEK cells ( $n = 16$  NPC-384 chips), in agreement with success rates reported by Zeng et al. (2008). This has posed a limitation in the use of fluoride-free, physiological internal solutions for high throughput APC and was the basis for the development of a special type of consumable, the NPC-384FF, which we have used throughout this study to allow the usage of K-gluconate (or K-chloride) or fluoride-based internal solutions under the same experimental conditions.

First, we evaluated the success rates for seal formation for fluoride-free internal solution compared with standard, fluoride-containing, internal solution using two standard cell culture cell lines. HEK cells expressing hERG as wells as CHO

cells expressing Nav1.5 channels were used on the SyncroPatch 384 using either NPC-384 chips and standard internal solution containing fluoride, or NPC-384FF chips with fluoride-free internal solution. For hERG, a classical double voltage-step protocol was used to record hERG tail currents and we determined the number of wells available for recording under both conditions. Using single-hole chips, HEK cells expressing hERG were recorded with a success rate of  $77.9 \pm 6.1\%$  ( $n = 10$  NPC-384 chips) for  $R_{\text{Seal}} > 1$  G $\Omega$  +  $I_{\text{Tail}} > 150$  pA (at the start of the experiment) when standard K-fluoride was used in the internal solution and  $35.9 \pm 7.9\%$  ( $n = 32$  NPC-384FF chips) when K-gluconate was used in the internal solution (Figure 1A). The success rate increased to  $87.2 \pm 5.4\%$  ( $n = 10$  NPC-384 chips) in K-fluoride and  $59.0 \pm 8.5\%$  ( $n = 32$  NPC-384FF chips) in K-gluconate when a QC cutoff for  $R_{\text{Seal}} > 0.25$  G $\Omega$  +  $I_{\text{Tail}} > 150$  pA was used. Despite the reduced number of available wells when fluoride-free solution was used, the sealing properties of the recorded cells only slightly differed in their  $R_{\text{Seal}}$  distribution pattern as illustrated in the histograms (Figure 1C), however, a small, but significant reduction for mean  $R_{\text{Seal}}$  values was observed (Table 2). Importantly, this did not have a large impact on the stability of the recording over time as only few cells were lost during the experiments and the success rate was similar at the end of the experiment ( $t = 15$  min) as at the start of the experiment (Figure 1A). The differences in mean  $R_{\text{Seal}}$  might be due to the fact that for the fluoride-free approach, the formation of CaF<sub>2</sub> crystals is absent and no elevated external Ca<sup>2+</sup> levels are used throughout the entire recording resulting in a reduced success rate. Similar results were observed using CHO cells expressing Nav1.5 channels where a 1-step voltage protocol was used to elicit Nav1.5 peak currents. Again, we first determined the number of available wells in single-hole chips (i.e., the number that passed the QC parameters for  $R_{\text{Seal}}$  and  $I_{\text{Peak}}$ ) and for Nav1.5-CHO we observed a success rate of  $78.0 \pm 4.9\%$  ( $n = 15$  NPC-384 chips) for  $R_{\text{Seal}} > 1$  G $\Omega$  +  $I_{\text{Peak}} < -100$  pA (at the start of the experiment) when K-fluoride was used in the internal solution

and  $41.9 \pm 8.6\%$  ( $n = 17$  NPC-384FF chips) when K-gluconate was used in the internal solution (Figure 1B). The success rate increased to  $86.1 \pm 6.4\%$  ( $n = 15$  NPC-384 chips) in K-fluoride and  $55.0 \pm 11.7\%$  ( $n = 17$  NPC-384FF chips) in K-gluconate when a QC cutoff  $R_{\text{Seal}} > 0.25 \text{ G}\Omega + I_{\text{Peak}} < -100 \text{ pA}$  was used. In line with our results with hERG-HEK cells, we observed a similar  $R_{\text{Seal}}$  distribution pattern for both conditions as illustrated in the histogram (Figure 1D) and a significant difference in mean  $R_{\text{Seal}}$  values for CHO cells in standard and fluoride-free conditions (Table 3). Similar to hERG-HEK, success rates remained stable over the time course of the experiment, any differences can probably be also attributed to the absence of  $\text{CaF}_2$  crystal formation as described above. Taken together, the results from both standard cell culture cell lines (HEK293 or CHO) expressing either  $\text{Na}_V1.5$  or hERG channels suggest that the fluoride-free approach can be used as an alternative to fluoride-containing internal solution in automated patch clamp experiments with reduced, but acceptable success rates. Therefore, our aim was to minimize experimental variability (such as recording solutions, voltage protocols, recording temperature, expression system, and culturing conditions) and provide a systematic comparison of biophysical and pharmacological parameters for four different targets depending on the internal solutions used.

## Effect of internal fluoride on currents, biophysical properties, and pharmacology of hERG expressed in HEK cells

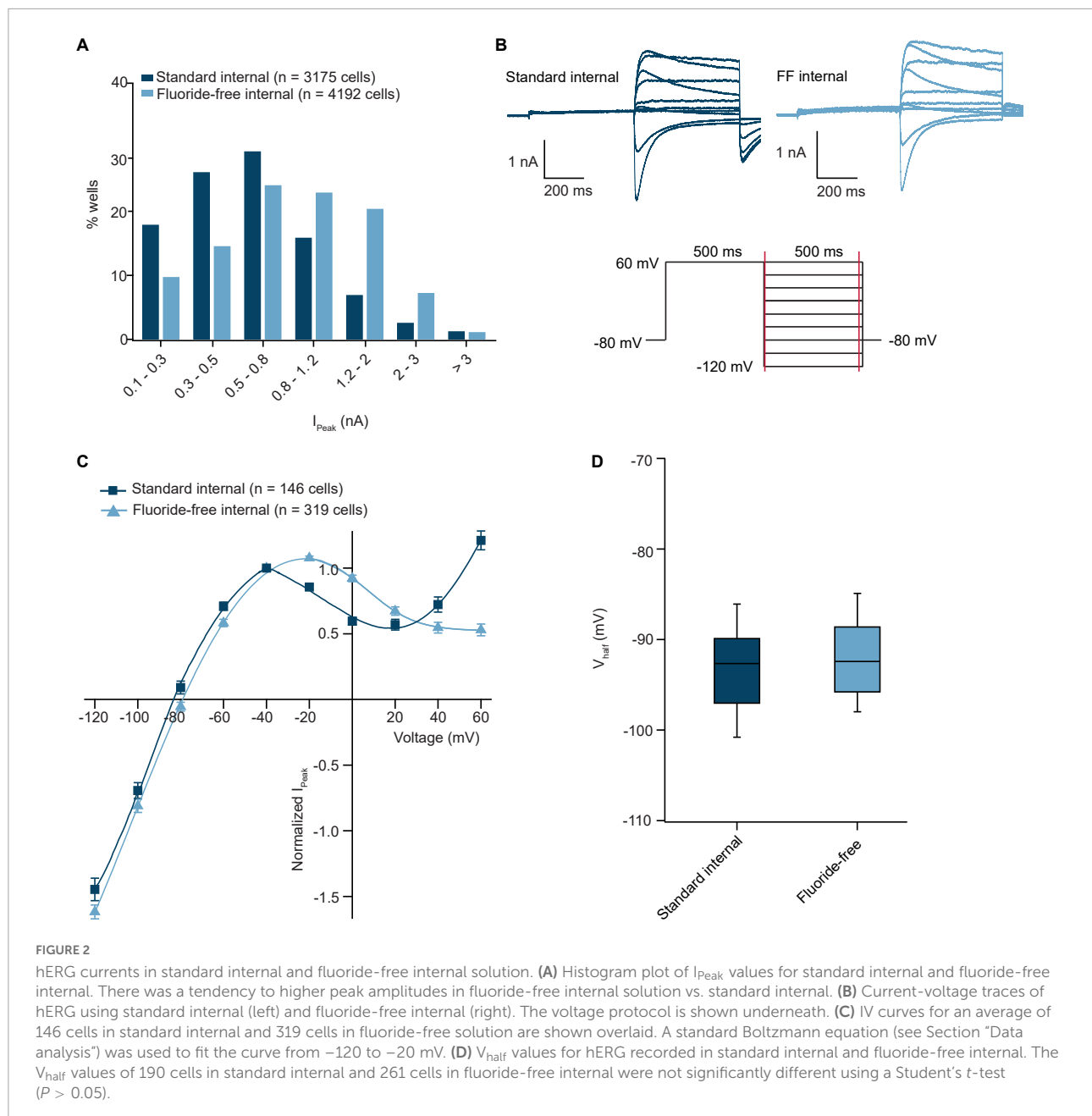
From the hERG-HEK recordings shown in Figures 1A,C we also extracted peak current levels from available wells as displayed in the histogram (Figure 2A). Interestingly, the data showed a difference in the distribution pattern in line with a significantly higher mean peak current level when using fluoride-free solution (Table 2) and single-hole chips. To further understand this difference, we examined the IV relationship using a classical double step inactivation protocol with increasing voltages after initial depolarization to +60 mV using standard and fluoride-free internal solution (Figure 2B) and found a similar IV-relationship that started to deviate for voltages more positive to -40 mV (Figure 2C). The currents were therefore normalized to -40 mV and fitted with a standard Boltzmann equation and resulted in  $V_{\text{half}}$  values of  $-93.0 \pm 0.5 \text{ mV}$  ( $n = 190$  cells) for standard and  $-92.1 \pm 2.3 \text{ mV}$  ( $n = 201$  cells) for fluoride-free internal solution with the data pools found to be not significantly different (Figures 2C,D and Table 2). The results imply that voltage dependence per se does not account for the difference in peak current level observed when fluoride-free solution was used. We can also rule out differences in cell size or access resistance as capacitance values were the same in both conditions and  $R_{\text{series}}$  values were

only slightly (but significantly) different (Table 2). Furthermore, the recordings were always performed in a comparable way on the same day using the same cells, recording temperature, external solution, and voltage protocol, with the only difference being the internal solution (standard or fluoride-free). This excludes any errors that may have arisen due to different recording conditions. Therefore, the reasons for the differences in increased currents in fluoride-free solution is unclear and further studies, such as detailed IV properties and a kinetic analysis, are required to elucidate the underlying reasons.

To investigate the influence of internal fluoride on the pharmacology of hERG channels we compared the  $\text{IC}_{50}$ s of verapamil and terfenadine in the presence and absence of internal fluoride. Figures 3A,B show traces from an example cell in the presence of increasing concentrations of verapamil in standard and fluoride-free internal solution, respectively. Figures 3C,D show the time course of the experiment for  $I_{\text{Tail}}$  current (at -40 mV) plotted over time using either standard (Figure 3C) or fluoride-free internal solution (Figure 3D) for an average of 54 and 11 cells, respectively. Also shown in Figures 3C,D is the vehicle control (0.3% DMSO,  $n = 58$  cells for standard internal solution and 12 cells for fluoride-free internal) where rundown was low for both groups, <2% over 18 min (Table 2) indicating  $I_{\text{Tail}}$  current amplitude was stable regardless of internal solution used ( $P = 0.7$ , Student's *t*-test). hERG was blocked by verapamil in a concentration-dependent manner with similar  $\text{IC}_{50}$ s and the concentration-response curves overlaid almost exactly (Figure 3E, for terfenadine, see Supplementary Figure 1). The spread of  $\text{IC}_{50}$ s for terfenadine and verapamil was higher when fluoride-free internal solution was used (Figure 3F) but the  $\text{IC}_{50}$ s were not different to those recorded in standard internal solution (Figure 3F and Table 2). Taken together, despite differences in tail current amplitude, hERG channel voltage dependence of inactivation, recording stability (rundown) as well as pharmacology for the compounds tested seem independent of whether fluoride-free or standard internal solution was used, which has also been suggested by other studies (Zeng et al., 2008) implying that the effect of internal fluoride might not be generalized per se and rather depends on subtype specific modulation of ion channel activity.

## Effect of internal fluoride on seal resistance, stability, biophysics, and pharmacology of $\text{Na}_V1.5$ expressed in CHO cells

From the experiments shown in Figures 1B,D, the peak current levels from available wells are displayed in Figure 4A as a histogram. In contrast to experiments involving hERG, the data showed a very similar distribution pattern consistent with a mean peak current amplitude that was not significantly different between the two groups ( $P = 0.2$ , Student's *t*-test; Table 3).



Furthermore, currents were stable during the time course of the experiment for both groups, with current rundown  $< 2\%$  over  $\sim 12$  min (Table 3). Next, we investigated the effect of internal fluoride on the voltage dependence of activation and fast inactivation. Looking at the literature, there is a relatively large variability in  $V_{half}$  values reported for  $Na_V1.5$  due to different experimental parameters including voltage protocol, recording solutions, co-expression with  $\beta$ -subunits, recording temperature, holding potential, or cell expression system, the values range from  $-25$  mV (Liu et al., 2003) to  $-50$  mV (McNulty and Hanck, 2004). For this reason, we kept

all experimental parameters the same, and only changed the internal solution in order to examine only the effect of fluoride on the  $V_{half}$  of activation and inactivation of  $Na_V1.5$ . Figure 4B shows the voltage protocols used for activation and inactivation of  $Na_V1.5$  channels with example traces for both conditions. The results of these experiments are illustrated in Figures 4C,D where the  $V_{half}$  of activation was  $-25.2 \pm 0.5$  mV ( $n = 241$ ) for fluoride-free and  $-37.5 \pm 0.4$  mV ( $n = 484$ ) for standard internal solution. A similar difference was observed for the  $V_{half}$  of inactivation with  $-53.6 \pm 0.6$  mV ( $n = 165$ ) in fluoride-free and  $-68.4 \pm 0.4$  mV ( $n = 728$ ) using standard internal

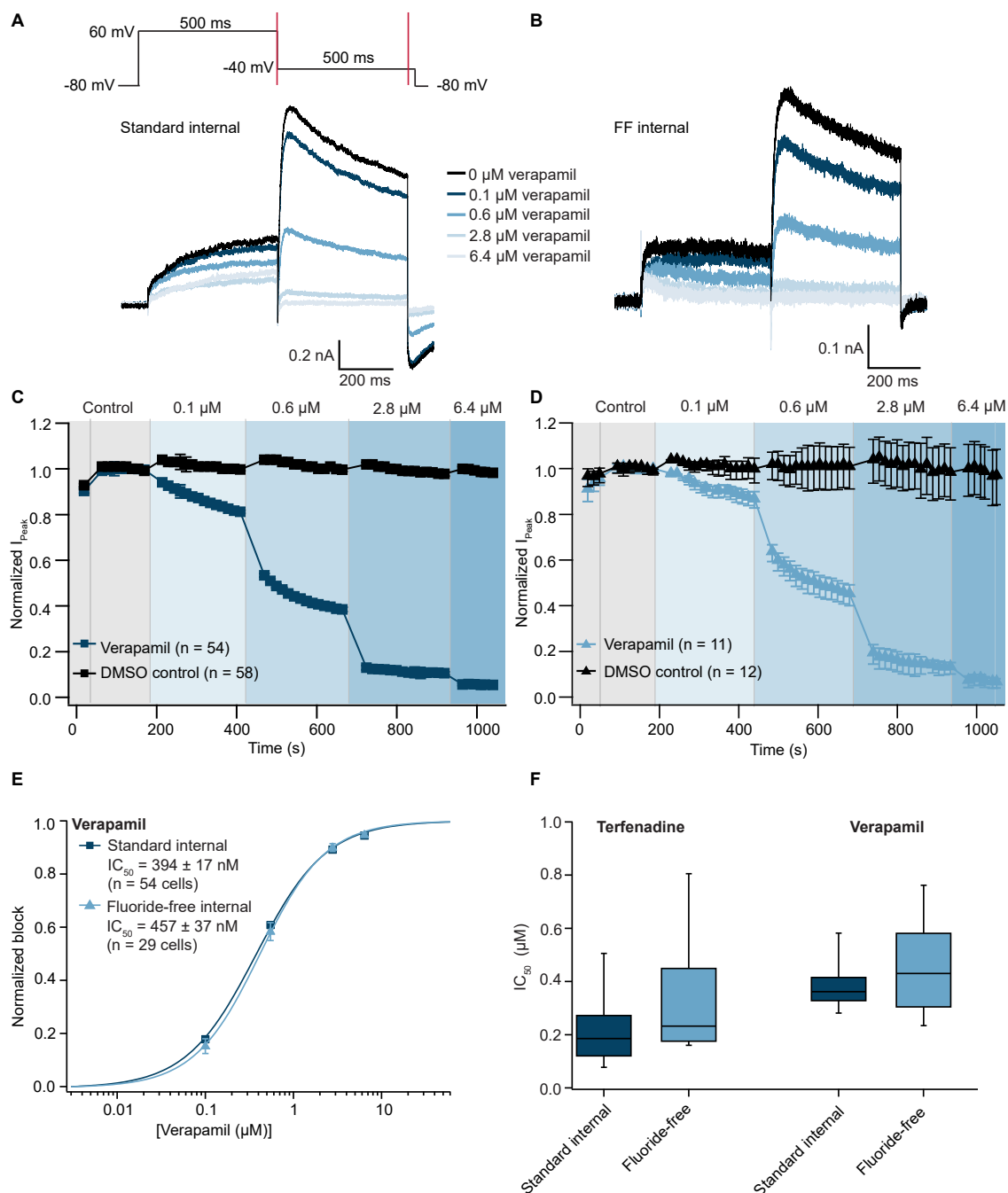
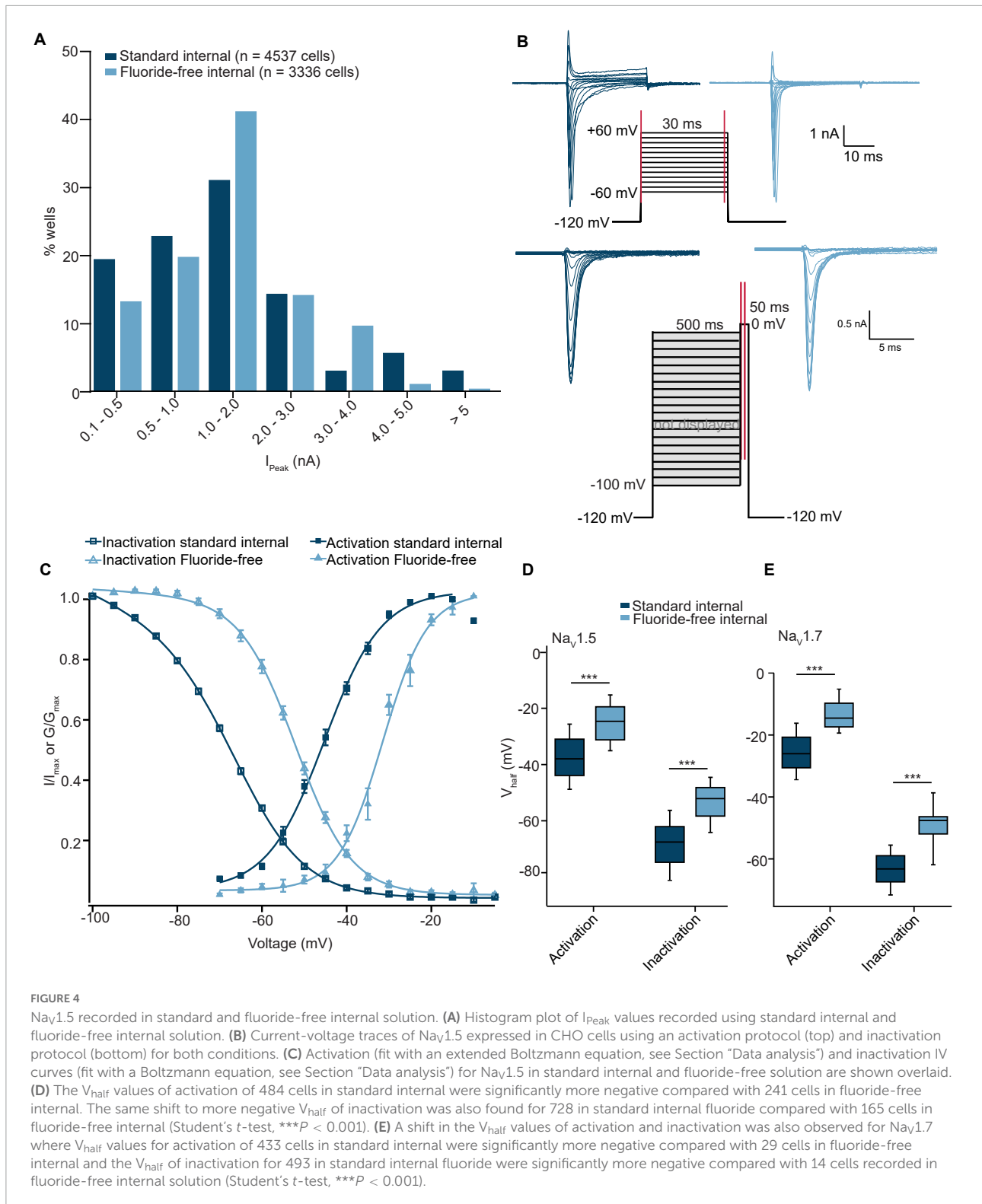


**FIGURE 3** Pharmacology of hERG recorded in standard and fluoride-free internal solution. **(A,B)** Raw current traces from an example HEK cell expressing hERG recorded in standard internal **(A)** and fluoride-free internal **(B)** solution was blocked by increasing concentrations of verapamil [voltage protocol is shown at the top of panel **(A)**]. **(C)** Corresponding time course of block by verapamil in standard internal **(C)** and fluoride-free internal **(D)**, 54 or 11 cells, respectively. Time course of 58/12 cells in DMSO control is also shown within panels **(C,D)**. **(E)** Concentration response curve for verapamil in standard internal solution or fluoride-free solution are shown overlaid. **(F)**  $IC_{50}$ s for terfenadine and verapamil recorded using standard internal or fluoride-free internal solution are shown as a box plot. The  $IC_{50}$ s for verapamil and terfenadine recorded in standard internal or fluoride-free internal solution were not significantly different using a Student's *t*-test ( $P > 0.05$ ).

solution. There is a clear hyperpolarizing effect of fluoride on the voltage sensitivity of Nav 1.5 channels which is highlighted in the boxplots shown in **Figure 4D** with  $\sim 12$  mV difference for  $V_{half}$

of activation and  $\sim 15$  mV for  $V_{half}$  of inactivation. Using the same voltage protocols as highlighted in **Figure 4B** we observed a similar hyperpolarizing shift for voltage activation/inactivation



of Na<sub>v</sub>1.7 expressed in CHO cells when standard K-fluoride internal solution was used. This suggests a common phenotype for the shift of voltage activation/inactivation in Na<sub>v</sub>1.5 and

Na<sub>v</sub>1.7 channels, however, further studies would be required to confirm whether other members of the Na<sub>v</sub> family are affected in a same manner. In fact, a previous report indicates sub-type

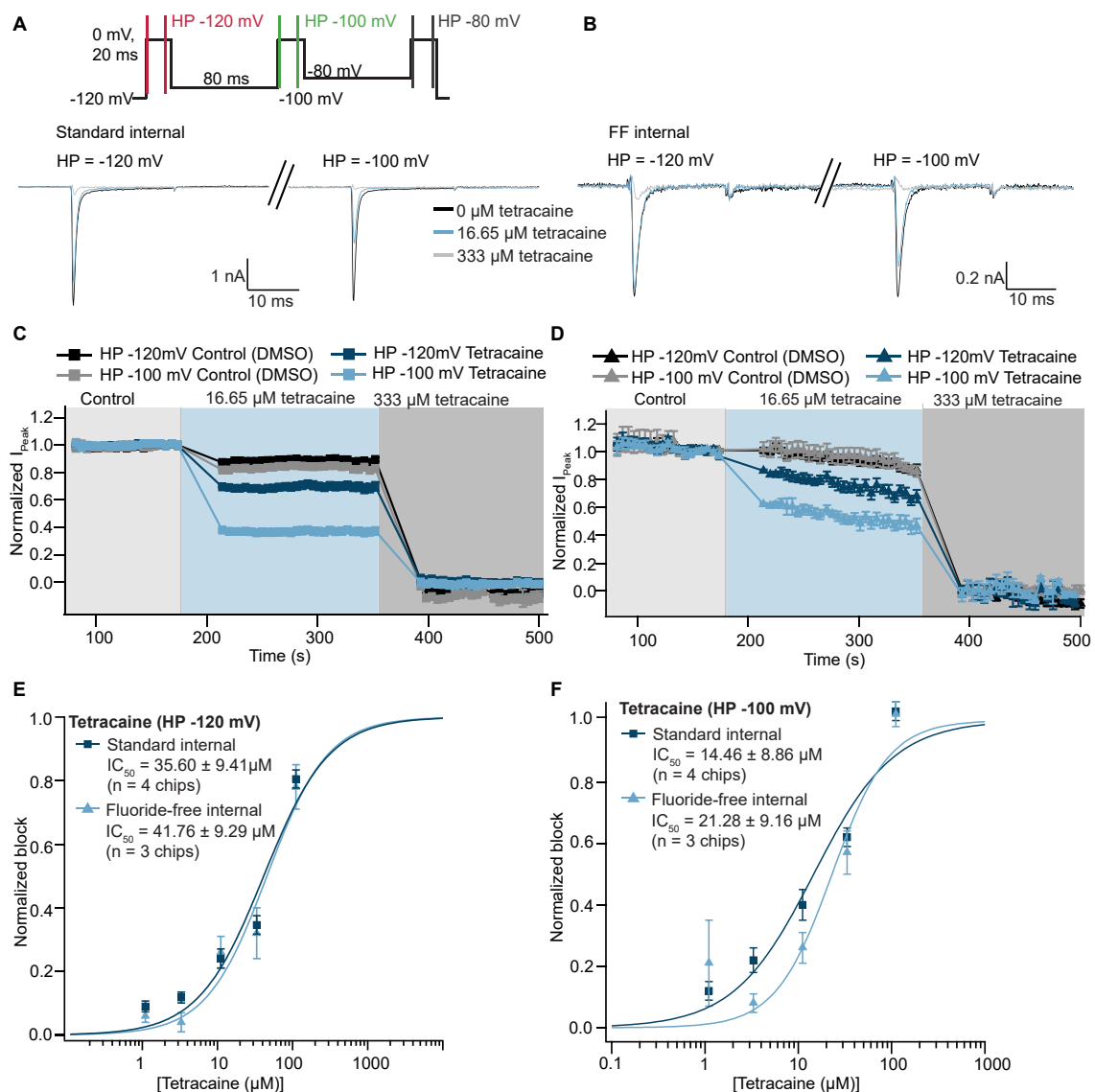


FIGURE 5

Pharmacology of  $Nav_{1.5}$  recorded in standard and fluoride-free internal solution. (A) Raw current traces from an example CHO cell expressing  $Nav_{1.5}$  recorded in standard internal solution were blocked by tetracaine using a 3-step protocol (voltage protocol shown at the top). Traces elicited by the first (holding potential -120 mV) and second (holding potential -100 mV) step are shown. (B) Raw current traces from an example CHO cell expressing  $Nav_{1.5}$  recorded in fluoride-free internal solution were blocked by tetracaine. (C) Corresponding time course of block by tetracaine in standard internal solution for an average of 23 wells (at different holding potentials), time course in DMSO for an average of 41 wells is also shown. (D) Corresponding time course of block by tetracaine in fluoride-free internal solution for an average of 10 wells (at different holding potentials), time course in DMSO for an average of 35 wells is also shown. (E) Concentration response curves for tetracaine in standard internal solution or fluoride-free solution at a holding potential of -120 mV are shown overlaid. (F) Concentration response curves for tetracaine in standard internal solution or fluoride-free solution at a holding potential of -100 mV are shown overlaid.

specific differences associated with the use of internal fluoride solutions (Coste et al., 2004).

To test whether fluoride influences pharmacology of  $Nav_{1.5}$  we used the known  $Nav$  channel blocker, tetracaine. This was applied as a single concentration of compound to each well, followed by a full block concentration (333 μM). Using a 3-Pulse protocol we were able to compare the block of  $Nav_{1.5}$ -mediated currents by tetracaine at three different holding

potentials as shown in Figures 5A,B (example traces are shown for the first two pulses only, corresponding to a holding potential of -120 and -100 mV). Figures 5C,D shows the peak current at 0 mV over time using two different holding potentials and tetracaine concentrations as well as vehicle only (0.3% DMSO) applied from the extracellular side. As expected, the potency of inhibition increased with a more depolarized holding potential for both conditions consistent with local

anesthetics preferably binding to the inactivated states (Hille, 1977; Hondeghem and Katzung, 1977; Bean et al., 1983; Li et al., 1999). Importantly, the concentration response curves for tetracaine overlaid almost exactly for individual voltages and were not statistically significantly different (Student's *t*-test,  $P > 0.05$ ) for 4 NPC-384 chips in standard internal and 3 NPC-384FF chips in fluoride-free internal solution. However, the  $IC_{50}$ s for tetracaine under both conditions decreased  $\sim 4$ – $7$  fold from holding potentials of  $-120$  mV compared with  $-100$  and  $-80$  mV (Figures 5E,F and Supplementary Table 1) comparable with values reported for lidocaine in the literature (Bean et al., 1983; Rapedius et al., 2019). In this way, the  $IC_{50}$  of tetracaine on  $Na_V1.5$  seems independent of whether fluoride is present or not, which is somewhat surprising given the clear hyperpolarizing effect of internal fluoride on voltage activation/inactivation of  $Na_V1.5$  (and  $Na_V1.7$ ) and the dependence of tetracaine  $IC_{50}$  on holding potential. Further studies are needed to elucidate the molecular mechanisms of these differences and how they apply to other compounds.

## Using fluoride-free solution to record $K_{Ca}3.1$ (SK4) channels in the presence of internal $Ca^{2+}$

We also tested the effect of internal fluoride for an ion channel activated by internal  $Ca^{2+}$  and used the internal perfusion of free  $Ca^{2+}$  to activate  $K_{Ca}3.1$  (SK4) channels. CHO cells expressing  $K_{Ca}3.1$  were captured with almost 50% success rate for  $R_{Seal} \geq 1$  G $\Omega$  with standard and fluoride-free internal solution (Figure 6A), if a QC cutoff of  $R_{Seal} \geq 0.25$  G $\Omega$  was used, the success rate was increased in both conditions (Figure 6A). As automated patch clamp recordings are sometimes performed using multi-hole chips to improve success of experiments, we also used multi-hole NPC-384 and NPC-384FF chips with 4 holes per well (4X). The success rates for cell capture and sealing were similar using 4X chips compared with single hole (1X) chips for both standard internal and fluoride-free internal solution (Figure 6A). Note that when 4X chips were used,  $R_{Seal} > 0.25$  G $\Omega$  is equivalent to  $R_{Seal} > 1$  G $\Omega$  with 1X chips and  $R_{Seal} > 0.05$  G $\Omega$  is equivalent to  $R_{Seal} > 0.25$  G $\Omega$  with 1X chips. A ramp voltage protocol from  $-120$  to  $60$  mV was applied from a holding potential of  $-80$  mV (Figure 6B). After exchange of the intracellular solution from  $0$  to  $1$   $\mu$ M free intracellular  $Ca^{2+}$  an outwardly rectifying current was observed that was inhibited by external application of  $1$  mM  $Ba^{2+}$  (Figures 6B,D) when standard internal or fluoride-free internal solution was used. In fact, we observed a slightly higher success rate for available wells that passed the quality control criteria for current ( $I > 350$  pA at  $60$  mV) after internal free  $Ca^{2+}$  application and  $R_{Seal} > 0.25$  G $\Omega$  before internal free  $Ca^{2+}$  application when fluoride-free solution was used (Figure 6C),  $70.3 \pm 6.9\%$  ( $n = 9$  chips) vs.  $60.6 \pm 9.4$  ( $n = 8$

chips) when standard internal solution was used. Interestingly, when we repeated the same experiment using 4X NPC-384FF chips (quality check criteria for current  $I > 1$  nA at  $60$  mV) the success rate increased to  $94.5 \pm 3.5\%$  ( $n = 2$  chips) and  $91.2 \pm 6.6$  ( $n = 2$  chips) when standard internal solution was used. This confirms the benefit of multi-hole chips for assay development in general, and as additional tool for experiments using fluoride-free internal solution.

Using increasing concentrations of internal free  $Ca^{2+}$ , we could estimate the apparent affinity for internal free  $Ca^{2+}$  to elicit  $K_{Ca}3.1$  currents (Figure 6E). Both inward (measured at  $-120$  mV) and outward currents (measured at  $60$  mV) were analyzed, and concentration response curves constructed for standard and fluoride-free solution at the different potentials. The concentration response curves for internal  $Ca^{2+}$  are shown overlaid in Figure 6E. The corresponding current analysis shows that when standard or fluoride-free solution was used, significantly larger peak currents were elicited at  $0.3$ ,  $1$ , and  $3$   $\mu$ M free internal  $Ca^{2+}$  compared with control ( $0$   $\mu$ M free internal  $Ca^{2+}$ ) recorded at  $60$  mV ( $P < 0.001$ ), whereas only  $1$  and  $3$   $\mu$ M free internal  $Ca^{2+}$  elicited a significantly larger peak amplitude compared with control ( $0$   $\mu$ M free internal  $Ca^{2+}$ ) recorded at  $-120$  mV ( $P < 0.001$ ), regardless of the internal solution used (Supplementary Figure 2). The data was normalized to the maximum response and fitted using a standard Hill equation (Figure 6E). The  $EC_{50}$  for internal  $Ca^{2+}$  was significantly lower when fluoride-free internal solution was used compared with standard internal solution at both  $60$  mV ( $635 \pm 20$  nM ( $n = 121$ ) vs.  $808 \pm 50$  nM ( $n = 66$ ;  $P < 0.01$ )) and  $-120$  mV ( $676 \pm 22$  nM ( $n = 121$ ) in fluoride-free solution vs.  $773 \pm 44$  nM ( $n = 66$ ) in standard internal ( $P < 0.05$ )).

We also determined the  $IC_{50}$  for external  $Ba^{2+}$  using either standard internal or fluoride-free internal at  $-120$  and  $60$  mV using 4X NPC-384 and 4X NPC-384FF chips, with the same ramp protocol shown in Figure 6B. Figure 6F shows the concentration response curves for  $Ba^{2+}$  at  $-120$  and  $60$  mV in standard and fluoride-free solution.  $Ba^{2+}$  was added as a single concentration to each well and the concentration response curves were constructed across the whole plate where it blocked the current at  $-120$  mV with a higher potency than at  $60$  mV. Figure 6F shows the average concentration response curves for 2 NPC-384 or 2 NPC-384FF chips. The  $IC_{50}$  for  $Ba^{2+}$  (mean  $\pm$  S.D.) was  $170 \pm 8$   $\mu$ M when standard and  $158 \pm 15$   $\mu$ M when fluoride-free internal solution was used at a voltage of  $-120$  mV. The  $IC_{50}$  increased  $\sim 3$ -fold to  $540 \pm 105$   $\mu$ M when standard and  $728 \pm 161$   $\mu$ M at  $60$  mV when fluoride-free internal solution was used.

From these results we conclude that the recording of  $Ca^{2+}$ -activated K-channels is possible under standard as well as fluoride-free conditions with similar success rates, and even higher success rates for available wells after  $Ca^{2+}$  activation with 4X chips than with 1X chips, making multi-hole chips a useful tool for recording  $Ca^{2+}$ -activated K-channels. Given

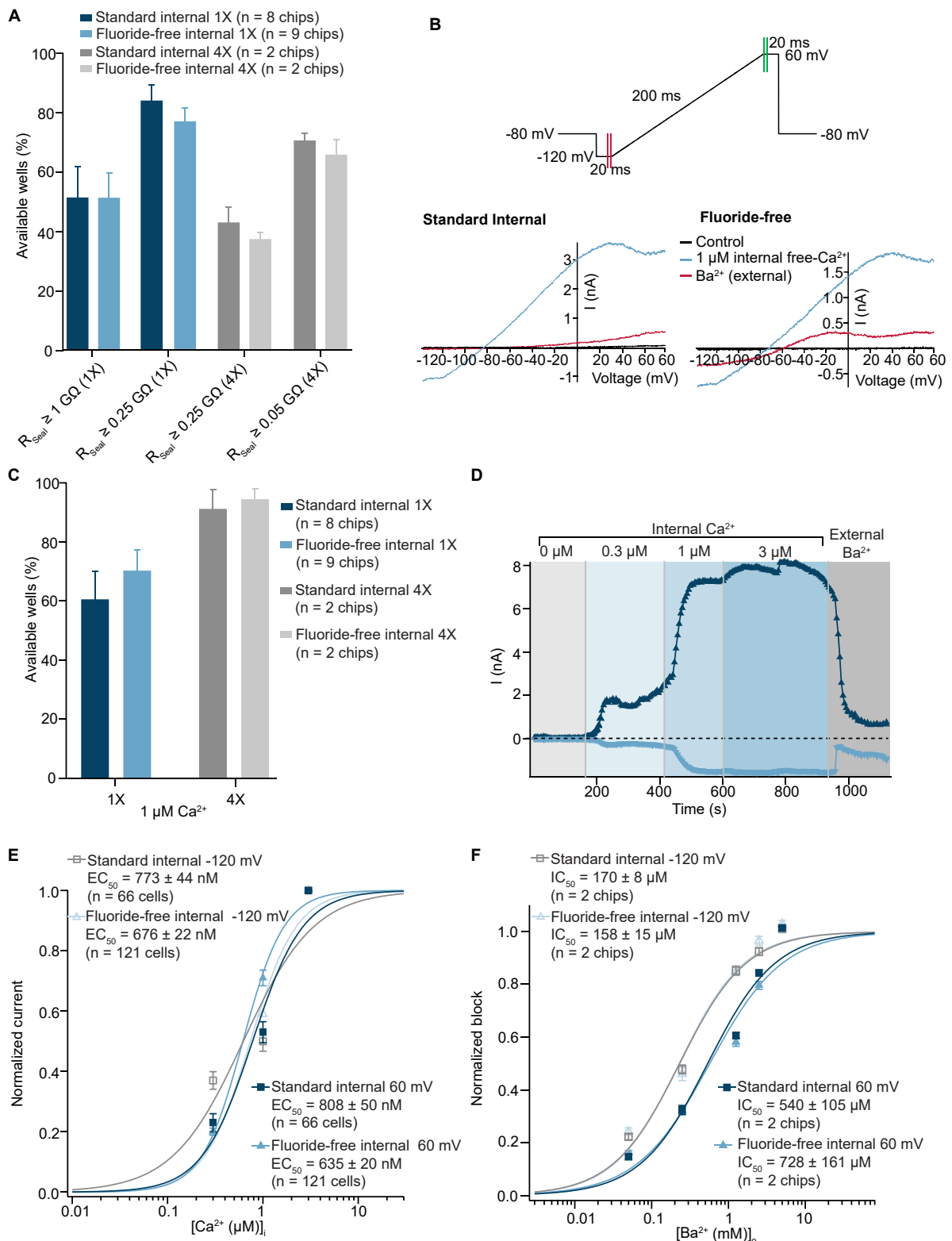


FIGURE 6

Activation by internal free  $\text{Ca}^{2+}$  of  $\text{KCa3.1}$  recorded in standard and fluoride-free internal solution. (A) CHO cells expressing  $\text{KCa3.1}$  were captured with almost 50% success rate for  $R_{Seal} \geq 1 \text{ G}\Omega$  with standard and in fluoride-free internal solution (left). If a QC cutoff of  $R_{Seal} \geq 0.25 \text{ G}\Omega$  was used, the success rate was increased in both conditions (right). Similar success rates were also achieved with multi-hole

(Continued)

FIGURE 6 (Continued)

(4X) chips (gray). (B) Raw current traces from example CHO cell expressing  $K_{Ca3.1}$  recorded in both standard and fluoride-free internal solution, activated by  $1 \mu\text{M}$  free internal  $\text{Ca}^{2+}$  and blocked by  $1 \text{ mM}$   $\text{Ba}^{2+}$  (external). (C) Success rates after applying initial  $R_{\text{Seal}} (>0.25 \text{ G}\Omega)$  and current QC plot of  $I_{\text{Peak}}$  values at  $-120/60 \text{ mV}$  for standard and fluoride-free solutions after internal application of  $1 \mu\text{M}$  free  $\text{Ca}^{2+}$ . (D) IT plot during application of internal free  $\text{Ca}^{2+}$  with  $0.3, 1,$  and  $3 \mu\text{M}$  free internal  $\text{Ca}^{2+}$  and subsequent block by external  $\text{Ba}^{2+}$  ( $1 \text{ mM}$ ) at  $-120/60 \text{ mV}$ . (E) Current values at  $-120$  or  $60 \text{ mV}$  in increasing concentrations of internal free  $\text{Ca}^{2+}$  were normalized to maximum peak amplitude and fit using a Hill equation which shows a slightly increased  $\text{EC}_{50}$  in standard internal solutions for both voltages. Shown are mean  $\pm$  S.E.M. (F) Current values at  $-120$  or  $60 \text{ mV}$  in increasing concentrations of external  $\text{Ba}^{2+}$  were normalized to maximum peak amplitude and fit using a Hill equation which showed no difference in the  $\text{IC}_{50}$  at  $-120 \text{ mV}$  between standard internal ( $170 \pm 8 \mu\text{M}, n = 2$  chips) and fluoride-free internal ( $158 \pm 15 \mu\text{M}, n = 2$  chips) or  $60 \text{ mV}$ , although the  $\text{IC}_{50}$  was higher at  $60$  vs.  $-120 \text{ mV}$  for both groups ( $540 \pm 105 \mu\text{M}, n = 2$  chips in standard external and  $728 \pm 161 \mu\text{M}, n = 2$  chips in fluoride-free internal solution).  $\text{IC}_{50}$  values are given as mean of 2 chips  $\pm$  S.D.

that the  $\text{EC}_{50}$  for  $\text{Ca}^{2+}$  was lower with fluoride-free internal solution, and peak currents were larger, we suggest that fluoride-free internal solution may provide an advantage over standard fluoride-containing internal solutions for recording  $\text{Ca}^{2+}$  activated channels.

## Discussion

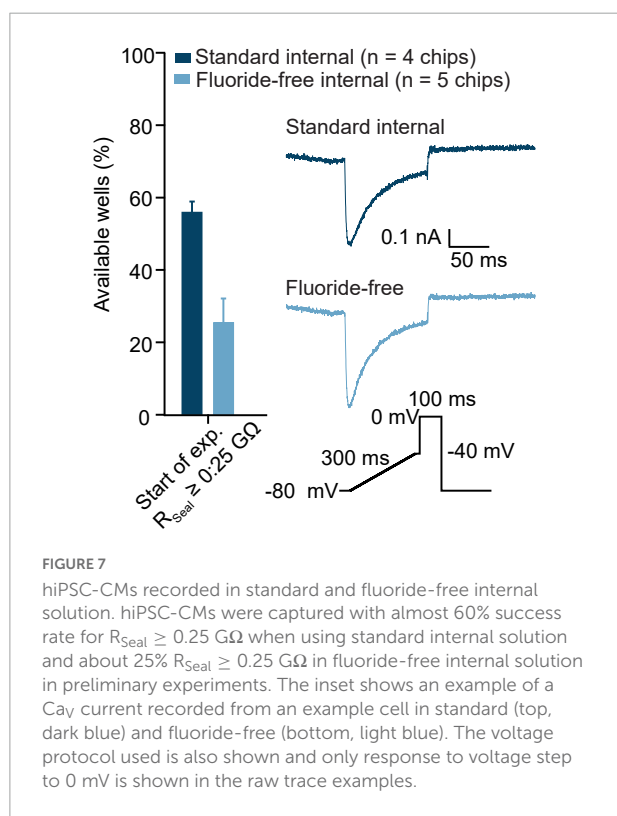
There is no doubt that automated patch clamp has become an integral part of many electrophysiological assays involving ion channels, including safety pharmacology, lead optimization, target validation, and channelopathy research (Obergrussberger et al., 2021, 2022). Unlike manual patch clamp, the cell cannot be chosen, nor can the patch clamp

aperture be moved to improve the seal. In APC, the patch clamp aperture is stationary and solely suction is used to attract the cell to the hole. In both manual and automated patch clamp, suction is then used to further improve the seal and to break into the whole cell configuration. Fluoride has been used in the internal solution in manual and automated patch clamp for years to assist with seal formation (Zeng et al., 2008; Föhr et al., 2021), in particular to record voltage-gated sodium channels where seal resistance and access parameters are critical for good voltage control. The mechanism is thought to involve  $\text{CaF}_2$  crystals forming at the aperture (Lojknér et al., 2019). However, it is well-documented that fluoride causes shifts in the activation and inactivation kinetics of  $\text{Na}_V$  channels (Meadows et al., 2002; Rugiero et al., 2003; Coste et al., 2004; Jarecki et al., 2008), as well as affecting persistent calcium current in neurons (Kay et al., 1986), activating G-proteins through interaction with  $\text{Al}^{3+}$  (Yatani and Brown, 1991; Li, 2003), and inhibits phosphatase activity (Khatra and Soderling, 1978).

## Fluoride has little effect on hERG currents

As expected, our data show that success rate as measured by % available wells using strict quality control parameters including  $R_{\text{Seal}} > 1 \text{ G}\Omega$  or  $0.25 \text{ G}\Omega$  and  $I_{\text{Peak}} > 150 \text{ pA}$  was higher when fluoride was used in the internal solution compared with fluoride-free internal solution when HEK cells stably expressing the hERG channel were used. However, with a success rate of around 60% for usable wells ( $R_{\text{Seal}} > 0.25 \text{ G}\Omega$ ) when K-gluconate was used, this results in over 200 usable wells in each experiment lasting approximately 20 min and thus, a vast increase in throughput compared with manual patch clamp. Importantly, there was little change in the number of usable wells at the end of the experiment compared with at the start, indicating that fluoride is not absolutely necessary for long-lasting recordings and 60% for completed experiments is an acceptable success rate for screening.

When fluoride was replaced by gluconate in the internal solution, hERG-mediated currents were slightly,



but statistically significantly, larger than when fluoride was present ( $P < 0.05$ , unpaired Student's  $t$ -test). This has not been previously reported and the reasons for the difference are not clear, additional studies are required to elucidate the underlying root cause. In our experiments, we can exclude differences in cell size since the cell capacitance values were unchanged in fluoride and fluoride-free solution, and we have also shown that fluoride does not shift the  $V_{\text{half}}$  of the hERG tail current. This is in agreement with Zeng et al. (2008, 2013) who also reported no effect on tail current activation parameters by fluoride compared with chloride when using the automated patch clamp system, the PatchXpress, and manual patch clamp, although the fluoride vastly increased success rate on the PatchXpress from 10% in K-chloride to 75% in K-fluoride (Zeng et al., 2008). Indeed, we also found no difference in success rate for K-chloride-containing internal solution compared with K-gluconate-containing internal solution (Supplementary Table 3) and can conclude that both gluconate and chloride are suitable alternatives to fluoride for recordings of hERG-HEK on the SyncroPatch 384.

We also compared the  $IC_{50}$  values for two compounds, terfenadine and verapamil, obtained using K-fluoride or K-gluconate and found that the  $IC_{50}$ s were not different and agreed well with the range found in the literature (Zeng et al., 2008; Kramer et al., 2013; Crumb et al., 2016; Brinkwirth et al., 2020). From our results and those of Zeng et al. (2008, 2013) we can conclude that fluoride does improve the success rate based on  $R_{\text{Seal}}$  and completed experiments and does not affect  $V_{\text{half}}$  of hERG tail current nor pharmacology, at least for the two compounds tested. Therefore, we can further conclude that the use of fluoride in the internal solution for hERG screening can be an advantage due to improved success rate, but fluoride-free internal solution can be used on the SyncroPatch 384 with success rates compatible with high throughput screening.

## Fluoride shifts $V_{\text{half}}$ of activation and inactivation of $Na_V1.5$ and $Na_V1.7$

CHO cells expressing  $Na_V1.5$  were also used on the SyncroPatch 384 in fluoride-free internal solution with similar success rates to HEK expressing hERG indicating that this method can be applied to different cell types and different ion channels. Average  $R_{\text{Seal}}$  values were  $>1 \text{ G}\Omega$  regardless of internal solution used, and no difference in  $I_{\text{Peak}}$  in fluoride-free internal solution compared with standard fluoride internal solution was observed which contrasts to the results observed with hERG.

Our results show that fluoride in the internal solution causes a negative shift in the  $V_{\text{half}}$  of activation and inactivation

of both  $Na_V1.5$  (Figures 4C,D) and  $Na_V1.7$  (Figure 4E) which agrees with previous reports that fluoride shifts the  $V_{\text{half}}$  of activation and inactivation to more negative values of  $Na_V1.3$  (Meadows et al., 2002),  $Na_V1.7$  (Jarecki et al., 2008), and  $Na_V1.9$  (Rugiero et al., 2003; Coste et al., 2004). The values for  $V_{\text{half}}$  of activation and inactivation for  $Na_V1.5$  and  $Na_V1.7$  were in good agreement with the literature for fluoride internal (Sheets and Hanck, 1999; Li et al., 2017). Importantly, despite shifts in the  $V_{\text{half}}$  of activation and inactivation, the  $IC_{50}$  of tetracaine block of  $Na_V1.5$  was not statistically different in fluoride-free internal solution compared with standard fluoride (Table 3 and Figures 5E,F). Changing the holding potential from  $-120$  to  $-100$  mV or  $-80$  mV resulted in a more potent  $IC_{50}$  of tetracaine, regardless of fluoride or fluoride-free internal solution was used (see Supplementary Table 1) as expected, as tetracaine and other local anesthetics are state dependent blockers of sodium channels (Hille, 1977; Hondeghem and Katzung, 1977; Bean et al., 1983; Li et al., 1999). The result is somewhat surprising given the fact that internal fluoride acts in a hyperpolarizing fashion and tetracaine is dependent on the holding potential used and may point towards related but independent mechanisms of modulation during transitions between closed, open and inactivated states of  $Na_V1.5$  channels as suggested for  $Na_V1.8$  and  $Na_V1.9$  channels (Coste et al., 2004).

A shift in the activation and inactivation kinetics for cardiac  $Na_V1.5$  channels over time has been reported for canine cardiac Purkinje cells (Hanck and Sheets, 1992), rat ventricular cardiac myocytes (Maltsev and Undrovinas, 1997), and rabbit atrial myocytes (Wendt et al., 1992) using manual whole cell patch clamp. In a small study using  $Na_V1.5$  expressed in CHO cells, our results also indicate a negative shift in the  $V_{\text{half}}$  of activation and inactivation over time (data not shown) as previously reported (Hanck and Sheets, 1992; Wendt et al., 1992; Maltsev and Undrovinas, 1997) when activation and inactivation IVs were measured after 10 min compared with immediately after achieving the whole cell configuration. The  $V_{\text{half}}$  of activation shifted by  $-0.78$  mV/min in fluoride internal and  $-0.43$  mV/min in fluoride-free internal solution. The  $V_{\text{half}}$  of inactivation shifted by  $-1.22$  mV/min in fluoride and  $-0.38$  mV/min in fluoride-free. In this respect, although the shift in parameters appeared to be more pronounced when fluoride was present, the absence of fluoride did not completely abolish this shift in agreement with Wendt et al. (1992) who also reported a shift in the activation and inactivation parameters regardless of whether fluoride, chloride, aspartate, or glutamate were present in the internal solution. It has been proposed that the shift in activation is dependent on the cytoskeleton (Maltsev and Undrovinas, 1997) and is prevented using the perforated patch technique (Wendt et al., 1992). All our experiments were performed in the whole cell mode of the

patch clamp technique, but the use of a perforator in the internal solution would allow perforated patch experiments to be performed.

Temperature has also been shown to affect activation and inactivation of  $\text{Na}_V$  channels where cooled temperatures cause a depolarizing shift in the  $V_{\text{half}}$  of activation of  $\text{Na}_V1.3$ , 1.5, 1.6, and 1.7 (Kriegeskorte et al., 2022). Increasing the temperature to physiological temperature ( $36 \pm 1^\circ\text{C}$ ) can also mildly shift the  $V_{\text{half}}$  of inactivation to more hyperpolarized potentials (Rotordam et al., 2021). Increased temperatures have also been shown to affect  $\text{IC}_{50}$ s on hERG current, e.g., erythromycin (Kirsch et al., 2004; Stoelzle et al., 2011) and  $\text{Na}_V1.5$ , e.g., mexiletine (Rotordam et al., 2021). For these reasons, it may be desirable to perform automated patch clamp experiments at physiological temperature. Recording at physiological temperature is more challenging and can result in a lower success rate and shorter recordings. In preliminary experiments at physiological temperature, we found that there was little change in the success rate when fluoride was used in the internal solution (see **Supplementary Table 2**) but the success rate in fluoride-free solution was slightly lower compared with room temperature [ $30.0 \pm 7.1$  (6 chips) for  $R_{\text{Seal}} > 1 \text{ G}\Omega$  at physiological temperature vs.  $41.9 \pm 8.6\%$  (17 chips) at room temperature see **Supplementary Table 2** and Section “High throughput APC to assess effects of internal fluoride on success rate and seal resistance”], nevertheless, and average  $R_{\text{Seal}}$  was  $> 1 \text{ G}\Omega$  in both conditions (**Supplementary Table 2**) and recordings lasted approximately 20 min (data not shown).

In conclusion for  $\text{Na}_V$  channels, we could confirm that fluoride shifts the  $V_{\text{half}}$  of activation and inactivation of  $\text{Na}_V1.5$  and  $\text{Na}_V1.7$  as has been reported for other  $\text{Na}_V$  channels (Meadows et al., 2002; Rugiero et al., 2003; Coste et al., 2004; Jarecki et al., 2008) but does not alter the  $\text{IC}_{50}$  of tetracaine on  $\text{Na}_V1.5$  channels. Success rates are higher when using fluoride in the internal solution, as expected, and many labs using both conventional and automated patch clamp use internal fluoride when recording  $\text{Na}_V$  channels and this must be taken into consideration when comparing kinetic parameters with the literature.

## Experiments involving $\text{Ca}^{2+}$ -activated ion channels

Intracellular  $\text{Ca}^{2+}$  activated ion channels pose a challenge to APC devices given the use of internal fluoride solutions and the very low solubility of  $\text{CaF}_2$  ( $K_{\text{sp}} = 3.5 \times 10^{-11}$ ) resulting in unstable amounts of free internal  $\text{Ca}^{2+}$  concentrations. Nevertheless, the use of appropriate buffer solutions and chelating agents do allow for the development of high throughput drug discovery on

$\text{Ca}^{2+}$ -activated K-Channels [please see Section “Materials and methods” (see **Table 1**) or Srinivasan et al. (2022)]. Our aim was to compare this approach to our recently developed fluoride-free method using a  $\text{Ca}^{2+}$ -activated K-channel.

When single hole chips were used, the success rate based on seal resistance did not differ much between standard and fluoride-free solutions, which contrasts to the success rate for cells expressing hERG or  $\text{Na}_V1.5$ , however, the success rate based on current amplitude after activation with  $1 \mu\text{M}$  internal free- $\text{Ca}^{2+}$  was increased in experiments where fluoride-free solution was used (**Figures 6A,C**). Additionally, current amplitudes were larger in fluoride-free internal solution (**Supplementary Figure 2**) and the  $\text{EC}_{50}$  for  $\text{Ca}^{2+}$  slightly lower (**Figure 6E**). Taken together, it would appear, for  $\text{Ca}^{2+}$ -activated ion channels at least, fluoride-free internal solution should be recommended. When fluoride is present, there is most probably an unknown amount of precipitation of  $\text{CaF}_2$ , even if this is not visible, and this can affect the apparent  $\text{Ca}^{2+}$  affinity, not to mention fluoride interfering with intracellular signaling process involving, for example, phosphorylation (Khatra and Soderling, 1978; Li, 2003). Activation of  $\text{Ca}^{2+}$ -activated K-channels using fluoride is possible on high throughput APC devices, as shown recently for the BK channel by Srinivasan et al. (2022), however, the free internal  $\text{Ca}^{2+}$  may be more stable in fluoride-free conditions, especially over time/during the course of the day where precipitation cannot be completely prevented. The use of multi-hole chips with four holes per well (4X) is also possible thus improving the success rate based on current amplitude for both standard and fluoride-free internal solution to over 90%.

## Conclusion

In keeping with the topic of this special issue: “Targeting Ion Channels for Drug Discovery: Emerging Challenges for High Throughput Screening Technologies,” we have overcome the challenge of low success rates and low seal resistances on high throughput automated patch clamp devices when using fluoride-free physiological internal solution. Implementation of specialized consumables (NPC-384FF) enables us to report success rates for fluoride-free recordings of approximately 60–80% for  $R_{\text{Seal}} \geq 0.25 \text{ G}\Omega$  and 40–50% for  $R_{\text{Seal}} \geq 1 \text{ G}\Omega$ . We mainly used a K-gluconate-based internal solution, but we observed similar success rates using K-chloride-based internal solution (**Supplementary Table 3**). Recordings were also stable, typically lasting around 20 min where cumulative additions of compound or single additions of compound and incubation times of 5 min in compound were used, as per best practice considerations recommended previously for hERG and  $\text{Na}_V1.5$  (Brinkwirth et al., 2020; Rotordam et al., 2021). In the case of hERG, since fluoride does not appear to exert an obvious influence over inactivation parameters or  $\text{IC}_{50}$  values, the user

is free to choose whether to use fluoride or fluoride-free internal solution and may prefer fluoride-containing solutions to maximize success rates and minimize cost per data point. For experiments involving  $\text{Na}_V$  channels, the user should be aware that fluoride causes shifts in activation and inactivation parameters and caution should be used when comparing data generated in different solutions. For recording  $\text{Ca}^{2+}$ -activated channels, success rates for completed experiments are similar under both conditions, however, the response to internal free  $\text{Ca}^{2+}$  and estimation of its apparent affinity may be more favorable to pursue when fluoride-free internal solution is used due to complete absence of  $\text{CaF}_2$  precipitation and, therefore, there is an advantage for the user to be able to utilize fluoride-free solution with success rates exceeding 50% for completed experiments. Coupling fluoride-free internal solution with multi-hole chips increases the success rate for available wells to >90% and is, therefore, also a consideration when designing the experiment in ion channel drug screening.

Additionally, in preliminary recordings we could successfully use the fluoride-free approach for experiments involving stem cell-derived cardiomyocytes (Figure 7). Therefore, the approach is not limited to standard cell lines but could be adopted for a wide range of cell types and experiments to bring conditions used to generate high throughput APC data closer and more comparable to recordings done using manual patch clamp and physiological solutions. Ultimately, this will enhance ion channel characterization and compound testing when using not only cell lines, but also induced pluripotent stem cells and primary cells.

## Data availability statement

The raw data supporting the conclusions of this article will be made available by the authors, without undue reservation.

## Author contributions

MR designed the study, performed the experiments and analysis, and contributed to writing and proofreading the manuscript. AO designed the experiments, analyzed the data, made the figures, and wrote and proofreading the manuscript. SS, TG, NB, and MGR performed the experiments and contributed to writing and proofreading the manuscript. IR-W, TS, and AR performed the experiments and analysis and contributed to writing and proofreading the manuscript. SF designed the study, performed analysis, and contributed to writing and proofreading the manuscript. NF contributed to writing and proofreading the manuscript. AL, FS, and NV provided the iPSC derived cardiomyocytes,

helped with the design of experiments, and contributed to writing and proofreading the manuscript. All authors contributed to the article and approved the submitted version.

## Funding

This work was supported by grants from the Deutsche Forschungsgemeinschaft (DFG) to NV (VO1568/3-1, VO1568/4-1, IRTG1816, and SFB1002 project A13 and under Germany's Excellence Strategy—EXC 2067/1—390729940) and from the German Center for Cardiovascular Research to NV (DZHK, 81X2300189, 81X4300102, 81X4300115, and 81X4300112).

## Acknowledgments

We thank SB Drug Discovery for kindly providing the hERG-HEK cell line and Charles River Laboratories for kindly providing the  $\text{Na}_V1.5$ -CHO,  $\text{Na}_V1.7$ -CHO, and  $\text{K}_{\text{Ca}3.1}$ -CHO cell lines used to compile this manuscript.

## Conflict of interest

MR, AO, SS, IR-W, TG, NB, MGR, TS, AR, SF, and NF were employed by Nanion Technologies, the manufacturers of the SyncroPatch 384 used to compile this manuscript. NF was a shareholder in Nanion Technologies. EH was employed by BioPharmaceuticals R&D, AstraZeneca.

The remaining authors declare that the research was conducted in the absence of any commercial or financial relationships that could be construed as a potential conflict of interest.

## Publisher's note

All claims expressed in this article are solely those of the authors and do not necessarily represent those of their affiliated organizations, or those of the publisher, the editors and the reviewers. Any product that may be evaluated in this article, or claim that may be made by its manufacturer, is not guaranteed or endorsed by the publisher.

## Supplementary material

The Supplementary Material for this article can be found online at: <https://www.frontiersin.org/articles/10.3389/fnmol.2022.982316/full#supplementary-material>

## References

- Bean, B. P., Cohen, C. J., and Tsien, R. W. (1983). 'Lidocaine block of cardiac sodium channels'. *J. Gen. Physiol.* 81, 613–642. doi: 10.1085/jgp.81.5.613
- Becker, N., Stoelzle, S., Göpel, S., Guinot, D., Mumm, P., Haarmann, C., et al. (2013). 'Minimized cell usage for stem cell-derived and primary cells on an automated patch clamp system'. *J. Pharmacol. Toxicol. Methods* 68, 82–87. doi: 10.1016/j.vascn.2013.03.009
- Becq, F., Mirval, S., Carrez, T., Lévêque, M., Billet, A., Coraux, C., et al. (2021). 'The rescue of F508del-CFTR by elxacaftor/tezacaftor/ivacaftor (Trikafta) in human airway epithelial cells is underestimated due to the presence of ivacaftor'. *Eur. Respir. J.* 59:2100671. doi: 10.1183/13993003.00671-2021
- Berger, H. A., Travis, S. M., and Welsh, M. J. (1998). 'Fluoride stimulates cystic fibrosis transmembrane conductance regulator Cl<sup>-</sup> channel activity'. *Am. J. Physiol. Lung Cell. Mol. Physiol.* 274, L305–L312.
- Billet, A., Froux, L., Hanrahan, J. W., and Becq, F. (2017). 'Development of automated patch clamp technique to investigate CFTR chloride channel function'. *Front. Pharmacol.* 8:195. doi: 10.3389/fphar.2017.00195
- Brinkwirth, N., Takasuna, K., Doi, M., Becker, N., Obergrussberger, A., Friis, S., et al. (2020). 'Reliable identification of cardiac liability in drug discovery using automated patch clamp: Benchmarking best practices and calibration standards for improved proarrhythmic assessment'. *J. Pharmacol. Toxicol. Methods* 105:106884. doi: 10.1016/j.vascn.2020.106884
- Brueggemann, A., George, M., Klau, M., Beckler, M., Steindl, J., Behrends, J. C., et al. (2004). 'Ion channel drug discovery and research: The automated nanopatch-clamp © technology'. *Curr. Drug Discov. Technol.* 1, 91–96. doi: 10.2174/1570163043484833
- Brüggemann, A., Farre, C., Haarmann, C., Haythornthwaite, A., Kreir, M., Stoelzle, S., et al. (2008). 'Planar patch clamp: Advances in electrophysiology,' in *Methods in molecular biology, potassium channels*, ed. J. D. Lippiat (Totowa, NJ: Humana Press, a part of Springer Science & Business Media), 165–176. doi: 10.1007/978-1-59745-526-8
- Brüggemann, A., Friis, S., Strassmeier, T., Goetze, T., Haarmann, C., Fertig, N., et al. (2017). Characterization of CFTR activators and inhibitors by the use of a planar patch clamp system. *Biophys. J.* 112:411a. doi: 10.1016/j.bpj.2016.11.2561
- Chen, Y. H., Dale, T. J., Xie, X. M., Clare, J. J., Romanos, M. A., Whitaker, W. R., et al. (2000). 'Cloning, distribution and functional analysis of the type III sodium channel from human brain'. *Eur. J. Neurosci.* 12, 4281–4289. doi: 10.1111/j.1460-9568.2000.01336.x
- Coste, B., Osorio, N., Padilla, F., Crest, M., and Delmas, P. (2004). 'Gating and modulation of presumptive Nav1.9 channels in enteric and spinal sensory neurons'. *Mol. Cell. Neurosci.* 26, 123–134. doi: 10.1016/j.mcn.2004.01.015
- Crumb, W. J., Vicente, J., Johannesen, L., and Strauss, D. G. (2016). 'An evaluation of 30 clinical drugs against the comprehensive in vitro proarrhythmia assay (CiPA) proposed ion channel panel'. *J. Pharmacol. Toxicol. Methods* 81, 251–262. doi: 10.1016/j.vascn.2016.03.009
- Cummins, T. R., Dib-Hajj, S. D., Black, J. A., Akopian, A. N., Waxman, S. G., Wood, J. N., et al. (1999). A novel persistent tetrodotoxin-resistant sodium current in SNS-null and wild-type small primary sensory neurons. *J. Neurosci.* 19:RC43. doi: 10.1523/jneurosci.19-24-j0001.1999
- Föhr, K. J., Nastos, A., Zimmer, T., Jungwirth, B., Messerer, D. A. C., Fauler, M., et al. (2021). 'Block of voltage-gated sodium channels by atomoxetine in a state- and use-dependent manner'. *Front. Pharmacol.* 12:622489. doi: 10.3389/fphar.2021.622489
- Froux, L., Elbahnsi, A., Boucherle, B., Billet, A., Baatallah, N., Hoffmann, B., et al. (2020). 'Targeting different binding sites in the CFTR structures allows to synergistically potentiate channel activity'. *Eur. J. Med. Chem.* 190:112116. doi: 10.1016/j.ejmech.2020.112116
- Hanck, D. A., and Sheets, M. F. (1992). Time-dependent changes in kinetics of Na<sup>+</sup> current in single canine cardiac Purkinje cells. *Am. J. Physiol. Heart Circ. Physiol.* 262(4 Pt 2), H1197–H1207. doi: 10.1152/ajpheart.1992.262.4.h1197
- Herrmann, A. M., Cerina, M., Bittner, S., Meuth, S. G., and Budde, T. (2020). 'Intracellular fluoride influences TASK mediated currents in human T cells'. *J. Immunol. Methods* 487:112875. doi: 10.1016/j.jim.2020.112875
- Hille, B. (1977). 'Local anesthetics: Hydrophilic and hydrophobic pathways for the drug-receptor reaction'. *J. Gen. Physiol.* 69, 497–515. doi: 10.1085/jgp.69.4.497
- Hondeghem, L. M., and Katzung, B. G. (1977). 'Time- and voltage-dependent interactions of antiarrhythmic drugs with cardiac sodium channels'. *BBA Rev. Biomembr.* 472, 373–398. doi: 10.1016/0304-4157(77)90003-X
- Jarecki, B. W., Jackson, J. O. II, Cummins, T. R., and Sheets, P. L. (2008). 'Paroxysmal extreme pain disorder mutations within the D3/S4-S5 linker of Nav1.7 cause moderate destabilization of fast inactivation'. *J. Physiol.* 586, 4137–4153. doi: 10.1113/jphysiol.2008.154906
- Kay, A. R., Miles, R., and Wong, R. K. S. (1986). 'Intracellular fluoride alters the kinetic properties of calcium currents facilitating the investigation of synaptic events in hippocampal neurons'. *J. Neurosci.* 6, 2915–2920. doi: 10.1523/jneurosci.06-10-02915.1986
- Khatri, B. S., and Soderling, T. R. (1978). 'Reversible inhibition of skeletal muscle phosphoprotein phosphatase by ATP, phosphate and fluoride'. *Biochem. Biophys. Res. Commun.* 85, 647–654. doi: 10.1016/0006-291X(78)91211-1
- Kirsch, G. E., Trepakova, E. S., Brimecombe, J. C., Erickson, H. D., Kochan, M. C., Shyja, L. M., et al. (2004). 'Variability in the measurement of hERG potassium channel inhibition: Effects of temperature and stimulus pattern'. *J. Pharmacol. Toxicol. Methods* 50, 93–101. doi: 10.1016/j.vascn.2004.06.003
- Kleinsorge, M., and Cyganek, L. (2020). 'Subtype-directed differentiation of human iPSCs into atrial and ventricular cardiomyocytes'. *STAR Protoc.* 1:100026. doi: 10.1016/j.xpro.2020.100026
- Kramer, J., Obejero-Paz, C. A., Myatt, G., Kuryshev, Y. A., Bruening-Wright, A., Verducci, J. S., et al. (2013). 'MICE models: Superior to the HERG model in predicting Torsade de Pointes'. *Sci. Rep.* 3:2100. doi: 10.1038/srep02100
- Kriegeskorte, S., Raya, B., Martin, H., Ralf, H., and Angelika, L. (2022). High-throughput electrophysiology reveals subtype specific temperature dependence of sodium channel activation and inactivation. *Biophys. J.* 121:95A. doi: 10.1016/j.bpj.2021.11.2249
- Li, H. L., Galue, A., Meadows, L., and Ragsdale, D. S. (1999). 'A molecular basis for the different local anesthetic affinities of resting versus open and inactivated states of the sodium channel'. *Mol. Pharmacol.* 55, 134–141. doi: 10.1124/mol.55.1.134
- Li, L. (2003). 'The Biochemistry and Physiology of Metallic Fluoride: Action, Mechanism, and Implications'. *Crit. Rev. Oral Biol. Med.* 14, 100–114. doi: 10.1177/154411130301400204
- Li, T., Lu, G., Chiang, E. Y., Chernov-Rogan, T., Chen, J., Grogan, J. L., et al. (2017). 'High-throughput electrophysiological assays for voltage gated ion channels using Syncro Patch 768PE'. *PLoS One* 12:e0180154. doi: 10.1371/journal.pone.0180154
- Liu, H., Atkins, J., and Kass, R. S. (2003). 'Common molecular determinants of flecainide and lidocaine block of heart Na<sup>+</sup> channels: Evidence from experiments with neutral and quaternary flecainide analogues'. *J. Gen. Physiol.* 121, 199–214. doi: 10.1085/jgp.20028723
- Lojknier, L. D., Anders, L., Rafael, S. D., and Roskva, R. K. (2019). 'Seal Enhancer'. *Copenhagen*. Available online at: <https://uspto.report/patent/app/20190383792> (accessed August 4, 2022).
- Maltsev, V. A., and Undrovinas, A. I. (1997). 'Cytoskeleton modulates coupling between availability and activation of cardiac sodium channel'. *Am. J. Physiol. Heart Circ. Physiol.* 273, H1832–H1840. doi: 10.1152/ajpheart.1997.273.4.h1832
- McNulty, M. M., and Hanck, D. A. (2004). 'State-dependent mibefradil block of Na<sup>+</sup> channels'. *Mol. Pharmacol.* 66, 1652–1661. doi: 10.1124/mol.66.6.1652
- Meadows, L. S., Chen, Y. H., Powell, A. J., Clare, J. J., and Ragsdale, D. S. (2002). 'Functional modulation of human brain Nav1.3 sodium channels, expressed in mammalian cells, by auxiliary  $\beta$ 1,  $\beta$ 2 and  $\beta$ 3 subunits'. *Neuroscience* 114, 745–753. doi: 10.1016/S0306-4522(02)00242-7
- Milligan, C. J., Li, J., Sukumar, P., Majeed, Y., Dallas, M. L., English, A., et al. (2009). 'Robotic multiwell planar patch-clamp for native and primary mammalian cells'. *Nat. Protoc.* 4, 244–255. doi: 10.1038/nprot.2008.230
- Obergrussberger, A., Friis, S., Brüggemann, A., and Fertig, N. (2021). 'Automated patch clamp in drug discovery: Major breakthroughs and innovation in the last decade'. *Exp. Opin. Drug Discov.* 16, 1–5. doi: 10.1080/17460441.2020.1791079
- Obergrussberger, A., Goetze, T. A., Brinkwirth, N., Becker, N., Friis, S., Rapedius, M., et al. (2018). 'An update on the advancing high-throughput screening techniques for patch clamp-based ion channel screens: Implications for drug discovery'. *Exp. Opin. Drug Discov.* 13, 269–277. doi: 10.1080/17460441.2018.1428555
- Obergrussberger, A., Haarmann, C., Rinke, I., Becker, N., Guinot, N., Brüggemann, A., et al. (2014). 'Automated patch clamp analysis of nACh $\alpha$ 7 and Nav 1.7 channels,' in *Current protocols in pharmacology*, ed. S. J. Enna (Hoboken, NJ: John Wiley & Sons Inc). doi: 10.1002/0471141755.ph113865
- Obergrussberger, A., Rinke-Weiß, I., Goetze, T. A., Rapedius, M., Brinkwirth, N., Becker, N., et al. (2022). 'The suitability of high throughput automated

patch clamp for physiological applications'. *J. Physiol.* 600, 277–297. doi: 10.1113/JP282107

Ono, K., and Arita, M. (1999). 'Mechanism of fluoride action on the L-type calcium channel in cardiac ventricular myocytes.'. *Cell Calcium* 26, 37–47. doi: 10.1054/ceca.1999.0050

Rapedius, M., Obergrussberger, A., Becker, N., Rinke-Weiß, I., Rotordam, M. G., et al. (2019) *High throughput pharmacology of Nav 1.5 channels on nanion's SyncroPatch 384PE*. Available online at: [https://www.nanion.de/images/phocadownloadpap/Application\\_Notes/Nanion\\_APP\\_Note\\_384PE\\_NaV1\\_5\\_06003.pdf](https://www.nanion.de/images/phocadownloadpap/Application_Notes/Nanion_APP_Note_384PE_NaV1_5_06003.pdf) (accessed June 27, 2022).

Renganathan, M., Cummins, T. R., Hormuzdiar, W. N., and Waxman, S. G. (2000). 'α-SNS Produces the slow TTX-resistant sodium current in large cutaneous afferent DRG neurons'. *J. Neurophysiol.* 84, 710–718. doi: 10.1152/jn.2000.84.2.710

Rotordam, M. G., Obergrussberger, A., Brinkwirth, N., Takasuna, K., Becker, N., Horváth, A., et al. (2021). 'Reliable identification of cardiac conduction abnormalities in drug discovery using automated patch clamp II: Best practices for Nav1.5 peak current in a high throughput screening environment'. *J. Pharmacol. Toxicol. Methods* 112:107125. doi: 10.1016/j.vascn.2021.10.7125

Rugiero, F., Mistry, M., Sage, D., Black, J. A., Waxman, S. G., Crest, M., et al. (2003). 'Selective expression of a persistent tetrodotoxin-resistant Na<sup>+</sup> current and Nav1.9 Subunit in myenteric sensory neurons'. *J. Neurosci.* 23, 2715–2725. doi: 10.1523/jneurosci.23-07-02715.2003

Seibert, F., Rapedius, M., Fakuade, F. E., Tomsits, P., Cyganek, L., Becker, N., et al. (2022). A modern automated patch-clamp approach for high throughput electrophysiology recordings in native cardiomyocytes. *Commun Biol.* (in press).

Sheets, M. F., and Hanck, D. A. (1999). 'Gating of skeletal and cardiac muscle sodium channels in mammalian cells'. *J. Physiol.* 514(Pt 2), 425–436.

Srinivasan, S. R., Huang, H., Chang, W.-C., Nasburg, J. A., Nguyen, H. M., Strassmaier, T., et al. (2022). Discovery of novel activators of large-conductance calcium-activated potassium channels for the treatment of cerebellar ataxia'. *Mol. Pharmacol.* 102, 17–28. doi: 10.1124/molpharm.121.00478

Stoelzle, S., Obergrussberger, A., Brüggemann, A., Haarmann, C., George, M., Kettenhofen, R., et al. (2011). 'State-of-the-art automated patch clamp devices: Heat activation, action potentials, and high throughput in ion channel screening'. *Front. Pharmacol.* 2:76. doi: 10.3389/fphar.2011.00076

Wendt, D. J., Starmer, C. F., and Grant, A. O. (1992). 'Na channel kinetics remain stable during perforated-patch recordings'. *Am. J. Physiol. Cell Physiol.* 263, C1234–C1240. doi: 10.1152/ajpcell.1992.263.6.c1234

Yatani, A., and Brown, A. M. (1991). 'Mechanism of fluoride activation of G protein-gated muscarinic atrial K<sup>+</sup> channels'. *J. Biol. Chem.* 266, 22872–22877. doi: 10.1016/s0021-9258(18)54435-5

Zeng, H., Balasubramanian, B., Penniman, J. R., Kinose, F., Salata, J. J., and Lagrutta, A. (2013). 'Halide ion effects on human ether-à-go-go related gene potassium channel properties'. *Assay Drug Dev. Technol.* 11, 544–550. doi: 10.1089/adt.2013.531

Zeng, H., Penniman, J. R., Kinose, F., Kim, D., Trepakova, E. S., Malik, M. G., et al. (2008). 'Improved throughput of PatchXpress hERG assay using intracellular potassium fluoride'. *Assay Drug Dev. Technol.* 6, 235–241. doi: 10.1089/adt.2007.116